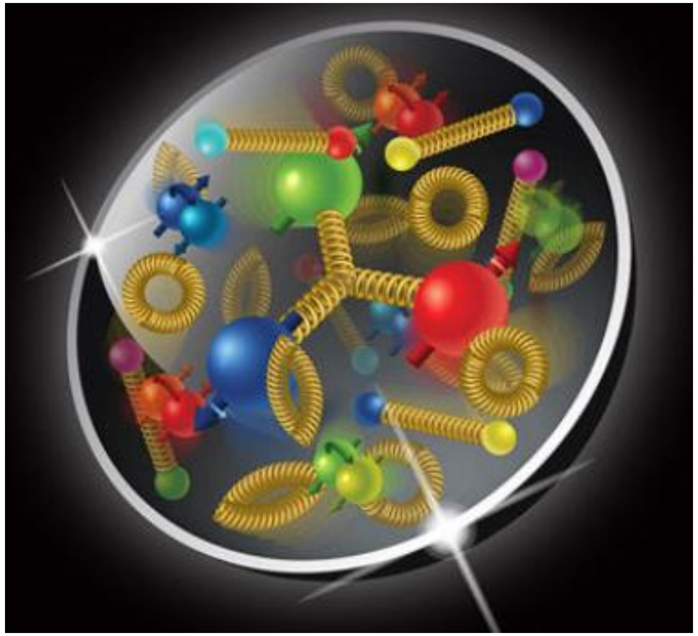

Hadronic scale, experimental point of view:

From high-energy lepton scattering to nucleon pressure

Lepton scattering on nucleon reveals the nucleon structure

Elastic Scattering: Form Factor and size of the nucleon

Deep Inelastic Scattering: Partons Distribution and momentum of partons

Exclusive Scattering: Generalized Parton Distributions

- ✓ **Correlation between position and momentum of partons**
- ✓ **Angular momentum and nucleon pressure**

Nicole d'Hose (Irfu, CEA Université Paris-Saclay)

Hadronic physics: from quarks to hadrons

Atomic physics	Nuclear Physics	Hadronic Physics	Particle Physics
10^{-10}m	10^{-14}m	10^{-15}m	10^{-18}m
			High Energy Physics

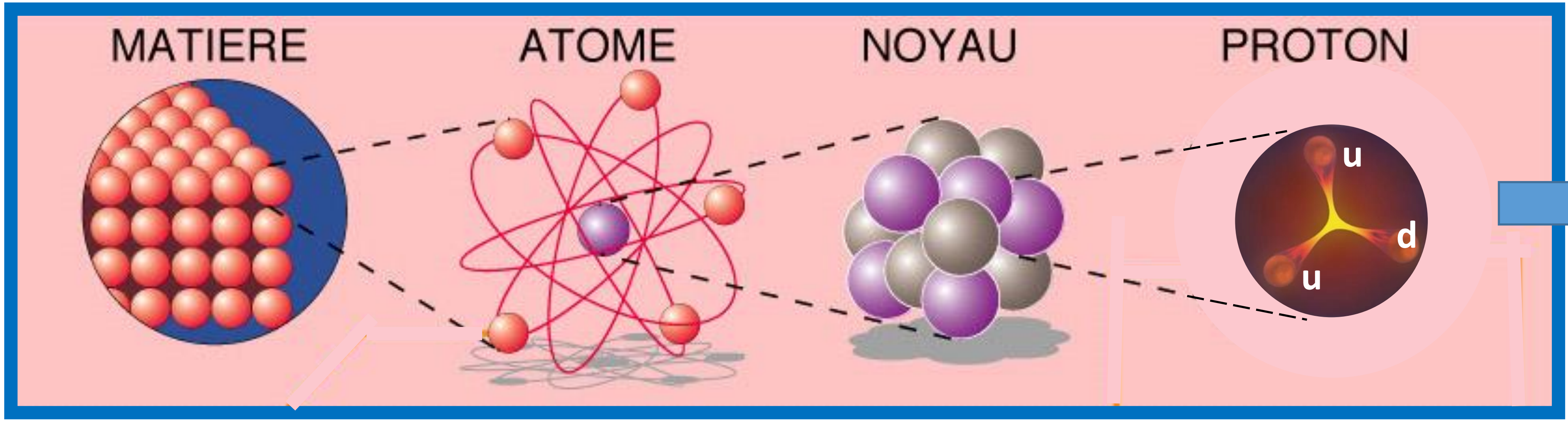

Quarks u, d

and gluons

quark mass:

u, d: mass < 5 MeV

s: mass < 100 MeV

c,b,t: mass 1 to 200 GeV

quark electric charge:

2/3 or -1/3 of e

massless gluons

Goal of hadronic physics:

Hadronic physics studies how hadrons, among which protons and neutrons constitute 99% of the mass of the visible universe, are composed and acquire their properties in terms of quarks and gluons, **the elementary fields of the Quantum Chromodynamics (QCD), the theory of strong interaction between quarks and gluons**

(Hervé's lecture to deal with QCD, numerical calculation on lattice, effective field theory…)

Hadronic physics: from quarks to hadrons

	Atomic physics	Nuclear Physics	Hadronic Physics	Particle Physics
	10^{-10}m	10^{-14}m	10^{-15}m	10^{-18}m
				High Energy Physics

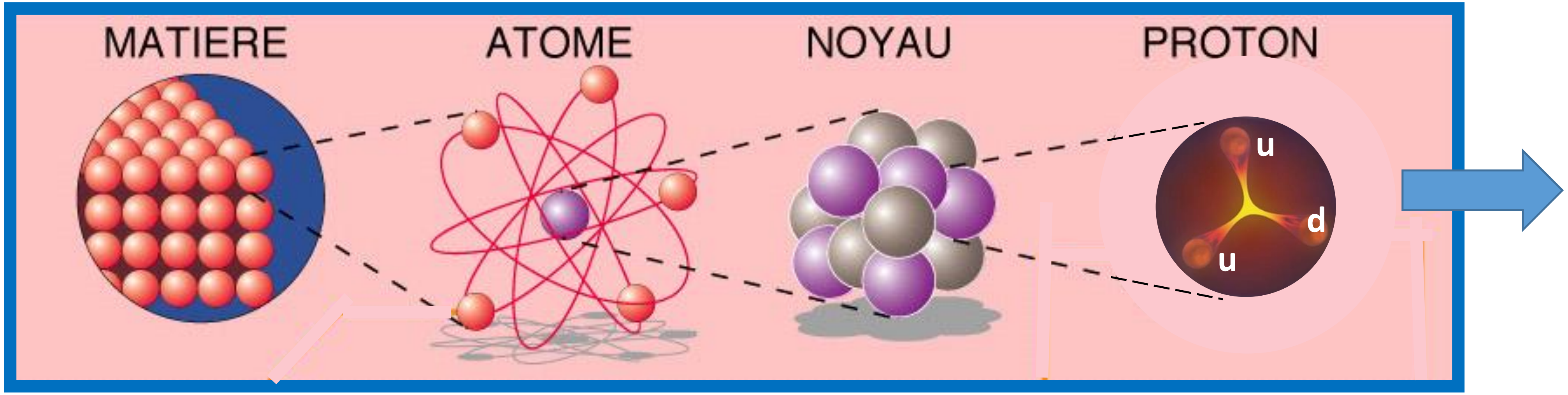

Quarks u, d

and gluons

quark mass:

u, d: mass < 5 MeV

s: mass < 100 MeV

c,b,t: mass 1 to 200 GeV

quark electric charge:

2/3 or -1/3 of e

massless gluons

Goal of hadronic physics:

Particles which undergo strong interaction are called **hadrons**

Hadrons are classified in **mesons** (bosons) and **baryons** (fermions)

- ✓ Why the lightest baryon, the proton, made up of massless gluons and almost massless quarks has a mass M_p=938 MeV?
- ✓ Why the lightest meson, the pion, has a mass M_{pion}=140 MeV ≈ 1/7 M_p?

➔ Mass, Energy, Pressure, *How are the forces distributed in space to make the proton a stable particle?*

A brief story of the particle discovery

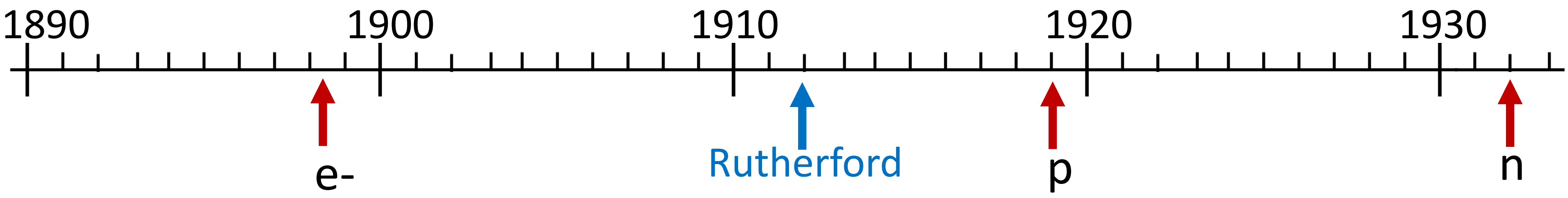

1932 Eisenberg proposed that
proton and **neutron** are manifestations of the same state: **the nucleon**

→ Introduction of isospin $I=1/2$ $I_3=\pm1/2$

1912 The Rutherford experiment

- By bombarding a very thin gold foil with alpha particles, Hans Geiger and Ernest Marsden, both students of Rutherford, observed that a small fraction (1 in 8000) of these particles were deflected at large angle as if it bounced off a heavy obstacle. The impacts were observed as scintillations in the dark, under the microscope, on a screen of zinc sulphide.

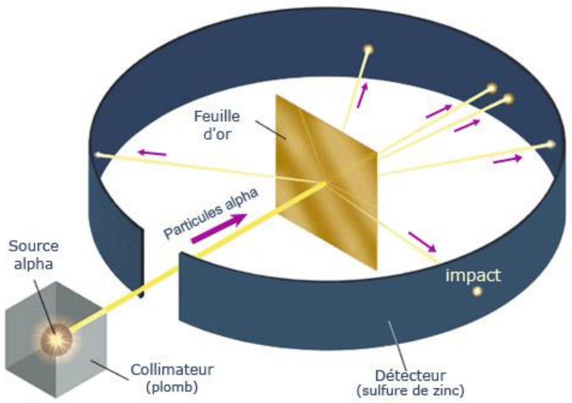

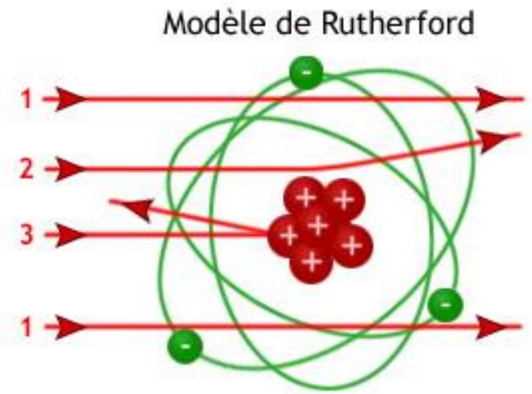

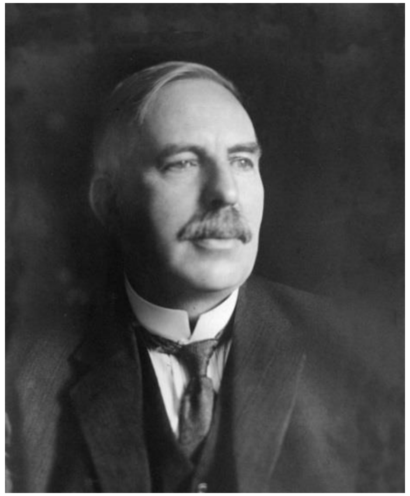

Typical experimental method in nuclear physics

- Projectile particles obey the Eisenberg relation : $\lambda\!\!\!^- = \hbar/P \leq$ size of the investigated object ($\hbar$=197 MeV fm)

Beam of α particles (m_α =3.7 GeV) of 5 MeV (classical mechanics) $P = \sqrt{(2m_\alpha E_c)}$ $\lambda\!\!\!^- = 197 / \sqrt{(2 \cdot 3700 \cdot 5)}$ fm = 1 fm

Beam of electrons (m_e =0.511 MeV) of 200 MeV (relativistic mechanics) $E^2 = P^2c^2 + m_e^2c^4$ $\lambda\!\!\!^- = 197 / 200$ fm = 1 fm

Point-like particule

Electromagnetic interaction QED

Probe momentum ↗ size of the observed details↘

A brief story of the particle discovery

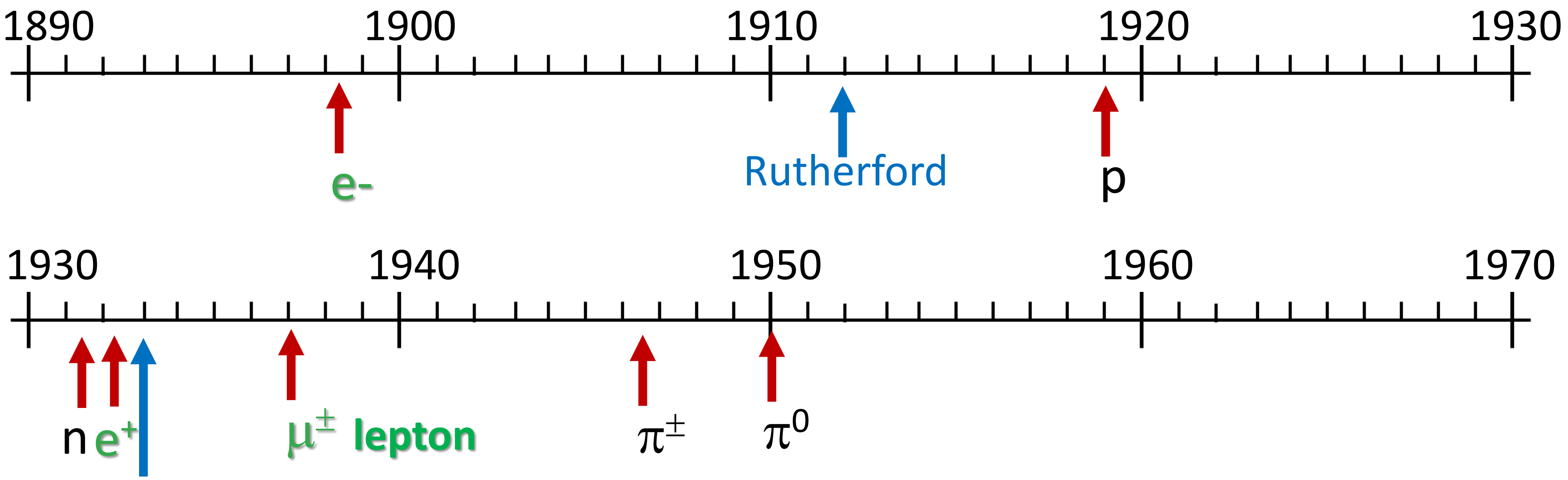

$\mu_p = 2.79\ e\hbar/2m_p = 2.79\ \mu_N$

$\mu_n = -1.91\ \mu_N$

The magnetic moment of the proton is 3 times larger than for a point-like particle

1950's: Hofstadter: elastic electron-proton scattering the cross section differs from that a point-like particle

➔ The proton has a size and a rich internal structure

lepton-proton elastic scattering

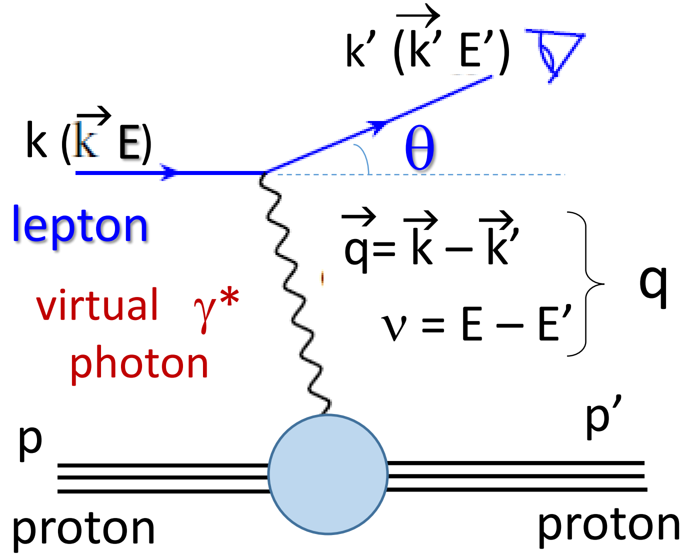

Hypotheses:

- ✓One photon exchanged
- ✓M_{e-} <<

for elastic case

$q^2 = (k-k')^2 \qquad = (p-p')^2 = \mathbf{t}$

$Q^2 = \nu^2 - |\vec{q}|^2 = -2k\cdot k' = -2\,E\,E' + 2\,E\,E'\cos\theta$

$Q^2 = \quad -q^2 \quad = \quad 4\,E\,E'\sin^2\theta/2 \;> 0$ in the lab.

$W^2 = (p+q)^2 = M_p^{\,2} - Q^2 + 2p.q$

$= M_p^{\,2} - Q^2 + 2M\upsilon$ for fixed target

$= M_p^{\,2}$ **for elastic case**

➔ $Q^2 = 2M\upsilon$

Elastic Scattering: e p → e′ p′

at fixed beam energy E, only one other variable

Q^2 (or υ) for theory $\qquad \upsilon = Q^2/2M$

θ (or E′) for experiment

$$E' = \frac{E}{1 + (2\,E/M_p)\sin^2\theta/2}$$

Form Factors (Q^2)

Nucleon radius (from $Q^2 \rightarrow 0$)

Form Factors of an extended and static object

''photographing'' an object by scattering an electron beam off is a well known technique to see its internal structure

$$\frac{d\sigma}{d\Omega} = \left(\frac{d\sigma}{d\Omega}\right)_{\text{point}} |F(q)|^2$$

$$F(q) = \int e^{i\vec{q}.\vec{r}} \rho(\vec{r})\, d^3\vec{r}$$

For a static target, the form factor is just the Fourier transform of the charge distribution

distribution sphérique $\rho(\vec{r}) = \rho(r)$.

$$F(q) = \int e^{i\,q.r.\cos\theta} \rho(r) r^2\, dr\, d\cos\theta\, d\varphi$$

$$F(q) = \frac{2\pi}{iq} \int \left[e^{i\,q.r.\cos\theta}\right]_{-1}^{+1} \rho(r)\, r\, dr \qquad \sin x = \frac{e^{ix} - e^{-ix}}{2i}$$

$$F(q) = \frac{4\pi}{q} \int_0^\infty \rho(r)\, \sin(qr)\, r\, dr$$

When q → 0 $\quad \sin qr = qr - \frac{(qr)^3}{6} + \ldots$

$$F(q) = \underbrace{\int_0^\infty 4\pi r^2 \rho(r)\, dr}_{1} - \frac{1}{6} q^2 \underbrace{\int_0^\infty r^2 \rho(r)\, 4\pi r^2\, dr}_{\langle r^2 \rangle} + \mathcal{O}(q^4)$$

$$F(q) = 1 - \frac{q^2}{6} \langle r^2 \rangle + \mathcal{O}(q^4)$$

$$\langle r^2 \rangle \equiv -6 \left. \frac{dF(q)}{dq^2} \right|_{q^2=0}$$

This is a definition

when q^2 ↗ phase shift $\delta = 2\pi\sqrt{\langle r^2 \rangle}/\lambda = 2\pi\sqrt{\langle r^2 \rangle}\, q/\hbar c$ ↗ F(q) ↘

and **the slope of the Form Factor at q^2=0 gives the spatial charge radius**

Form Factors and charge distribution

$$F(q) = \int e^{i\vec{q}.\vec{r}}\,\rho(\vec{r})\,d^3\vec{r}$$

Charge distribution $\rho(r)$	Form Factor $F(\boldsymbol{q}^2)$
$\delta(r)/4\pi$	1
$(a^3/8\pi)\cdot\exp(-ar)$	$(1+\boldsymbol{q}^2/a^2\hbar^2)^{-2}$
$(a^2/2\pi)^{3/2}\cdot\exp(-a^2r^2/2)$	$\exp(-\boldsymbol{q}^2/2a^2\hbar^2)$
$\begin{cases} 3/4\pi R^3 & \text{for } r \le R \\ 0 & \text{for } r > R \end{cases}$	$3\,\alpha^{-3}(\sin\alpha - \alpha\cos\alpha)$ with $\alpha = \lvert\boldsymbol{q}\rvert R/\hbar$

from: B. Povh, Particles and Nuclei

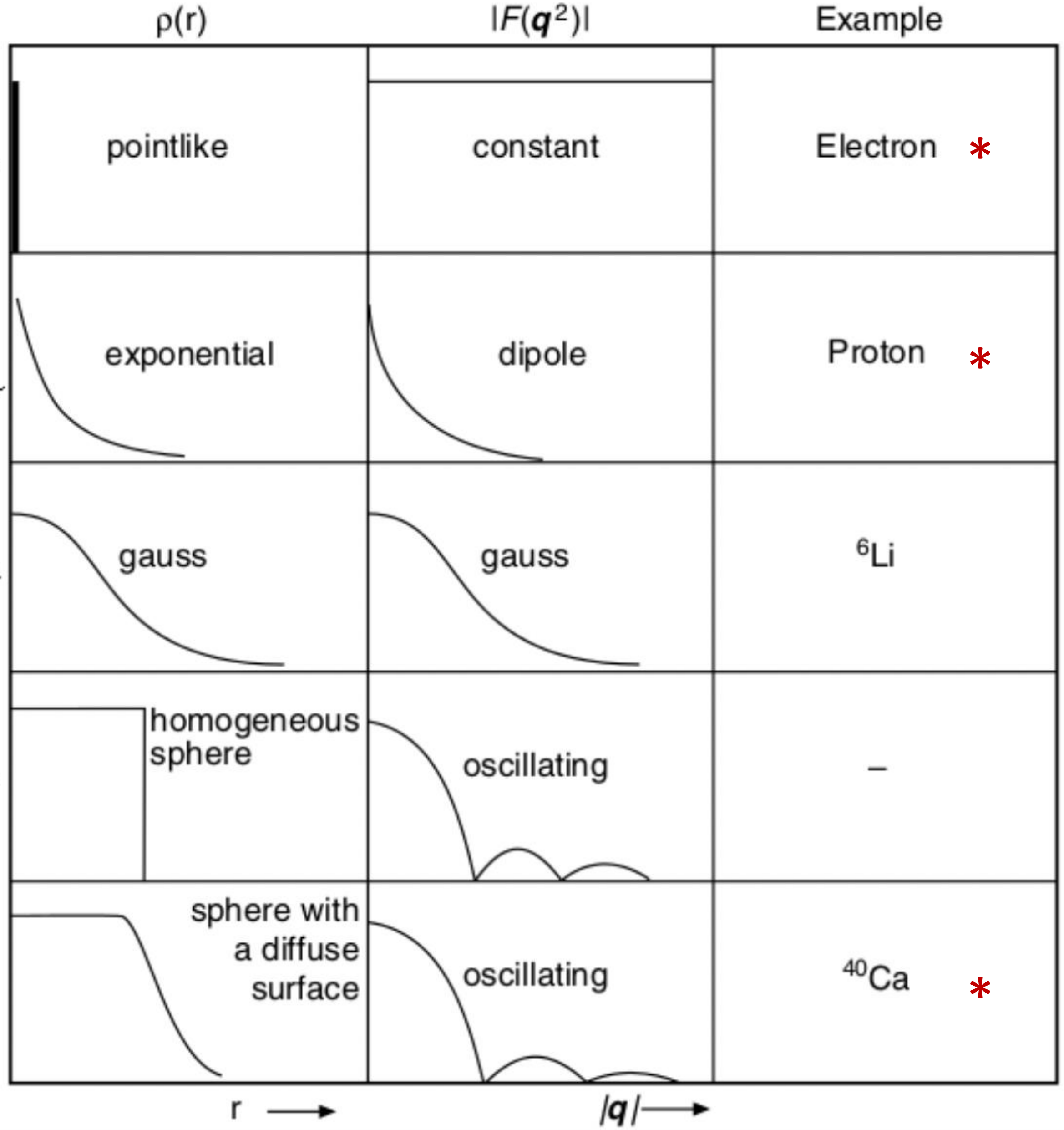

Electron scattering on Pb

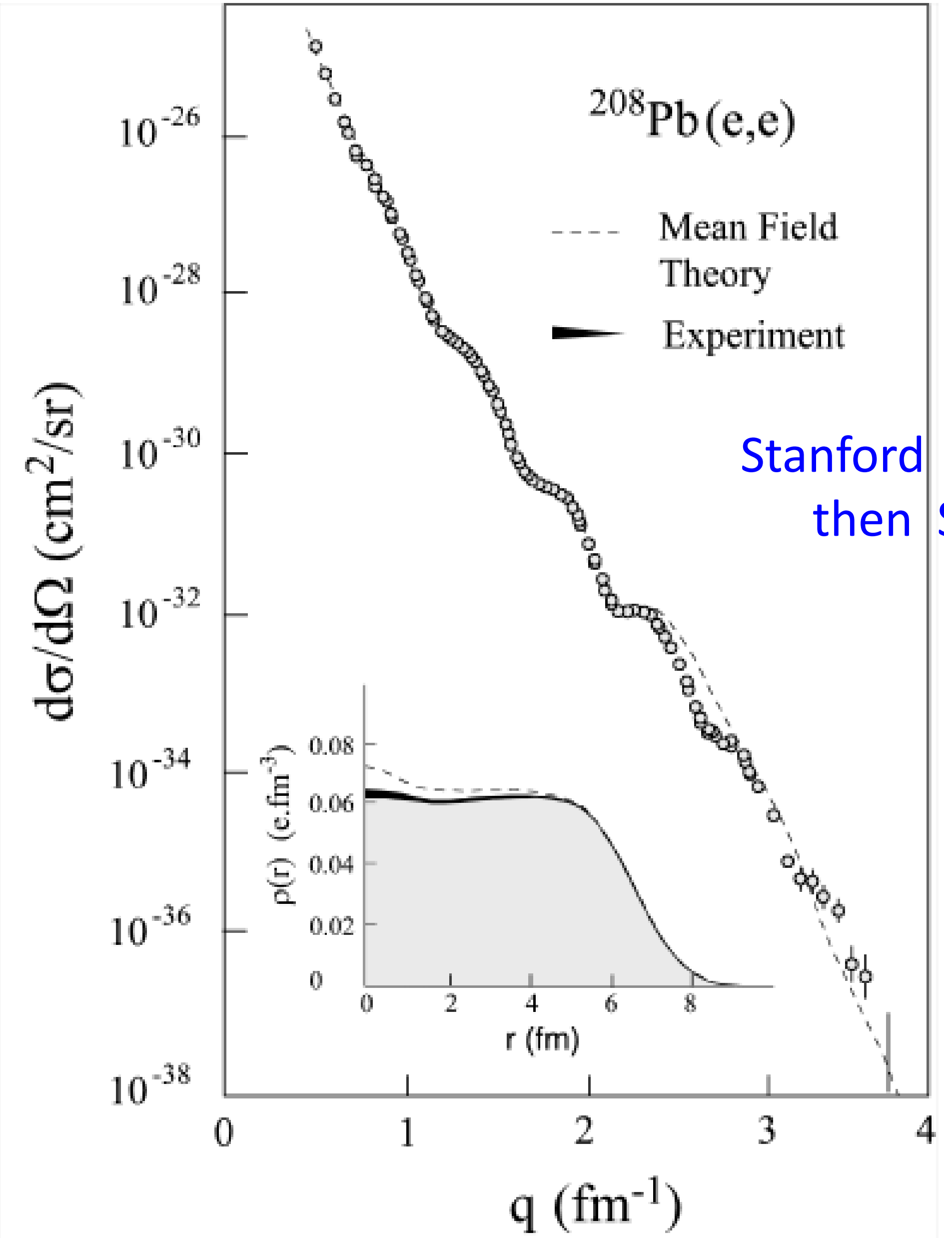

Stanford SLAC 1969 up to $q=2.7\ fm^{-1}$
then Saclay ALS 1976

Measurement with a great precision over 13 orders of magnitude

Electron scattering on a "proton" step by step

$$\left(\frac{d\sigma}{d\Omega}\right)_{lab} = \frac{\alpha^2}{4k^2\sin^4(\theta/2)}$$

Rutherford cross section of a spinless electron on a spinless target of infinite mass

$$\left(\frac{d\sigma}{d\Omega}\right)_{lab} = \frac{\alpha^2}{4k^2\sin^4(\theta/2)}\cos^2(\theta/2)\frac{E'}{E}$$

Mott cross section of an electron of spin ½ on a recoiling target of spin 0

$\cos^2(\theta/2)$ → spin ½ electron

$$\left(\frac{d\sigma}{d\Omega}\right)_{lab} = \frac{\alpha^2}{4k^2\sin^4(\theta/2)}\cos^2(\theta/2)\frac{E'}{E}\;[1 + 2\tau\tan^2(\theta/2)]$$

Rosenbluth cross section of an electron of spin ½ on a recoiling muon of spin ½

1 → Electric interaction with the charge e of the muon

$2\tau\tan^2(\theta/2)$ → Magnetic interaction with the spin ½ of the muon

$\tau = Q^2/4M^2$

ep → ep

$$\left(\frac{d\sigma}{d\Omega}\right)_{lal} = \sigma_{Mott}\left[F_1^2 + \tau F_2^2 + 2\tau(F_1+F_2)^2\tan^2\frac{\theta}{2}\right] = \sigma_{Mott}\left[\frac{G_E^2+\tau G_M^2}{1+\tau} + 2\tau G_M^2\tan^2\frac{\theta}{2}\right]$$

		proton	neutron	
Dirac FF: $F_1(Q^2=0)$ =	charge (in e unit)	1	0	$G_E(Q^2) = F_1(Q^2) - \tau F_2(Q^2)$
Pauli FF: $F_2(Q^2=0)$ =	anomalous magnetic moment κ	+1.79	-1.91	$G_M(Q^2) = F_1(Q^2) + F_2(Q^2)$

$\mu = (1+\kappa)\, e\hbar/2M$

1954-58 at Stanford electron scattering by Hofstadter

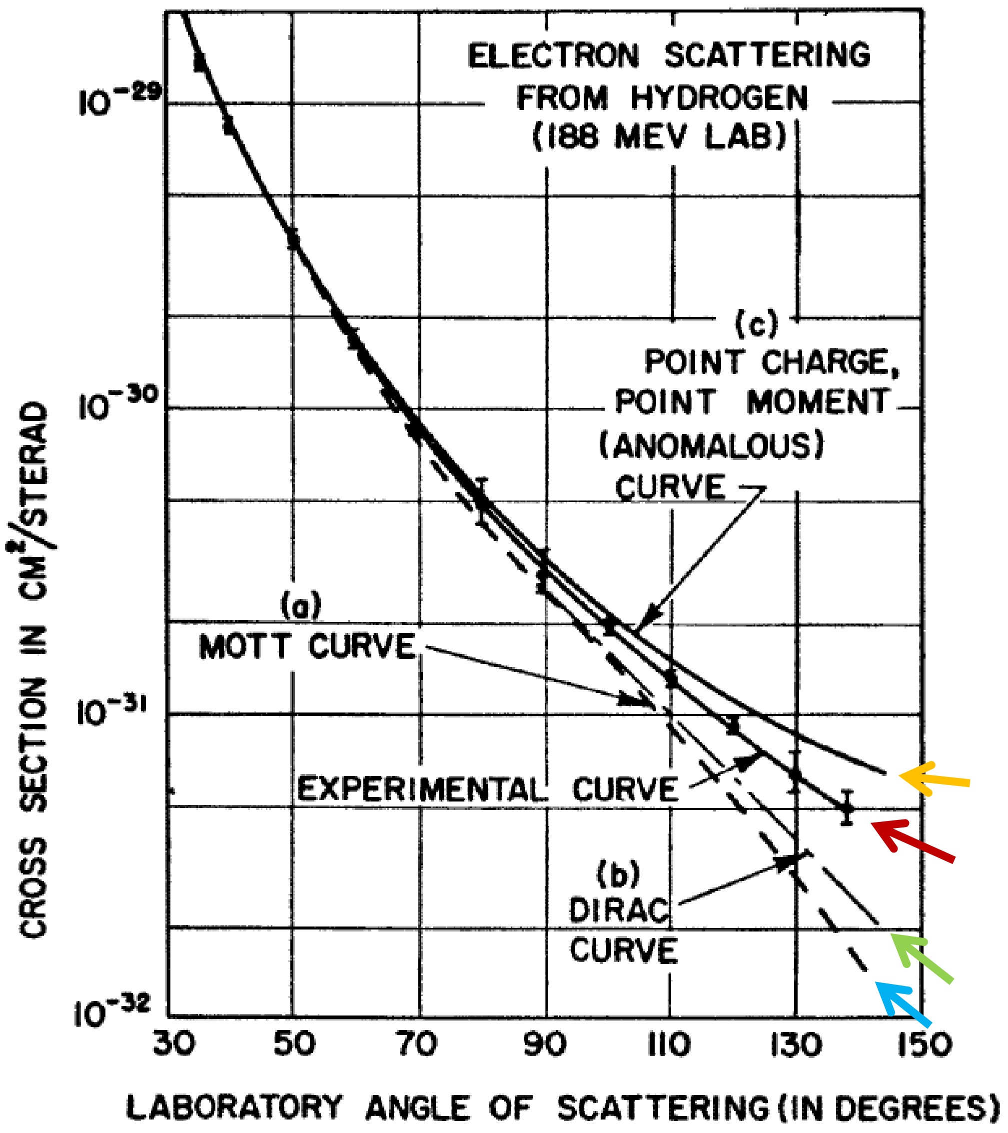

(a) Mott curve for spinless point-like proton

(b) Rosenbluth curve for a point-like proton
with a charge
but without anomalous magnetic moment
$F_1(q^2)=1$ and $F_2(q^2)=0$

(c) Rosenbluth curve for a point-like proton
with a charge
and with anomalous magnetic moment
$F_1(q^2)=1$ and $F_2(q^2)=\kappa$

➔ The deviation of the experimental data from a point-like proton indicates an effect from the proton form factors due to the proton finite size.

From Hofstadter *et al.,* Review of Modern Physics, Vol 30, 1958

1954-58 at Stanford electron scattering by Hofstadter

Robert Hofstadter
Nobel Prize 1961

MARKIII at Stanford
Electron beam E=100-600 MeV
Stanford Linear Accelerator Center
High Energy Physicis Laboratory
Duty cycle less than 1%

Typical experiment:
- Hydrogen and helium (gas) targets
- Magnetic spectrometer
- Measurements of scattering angle a

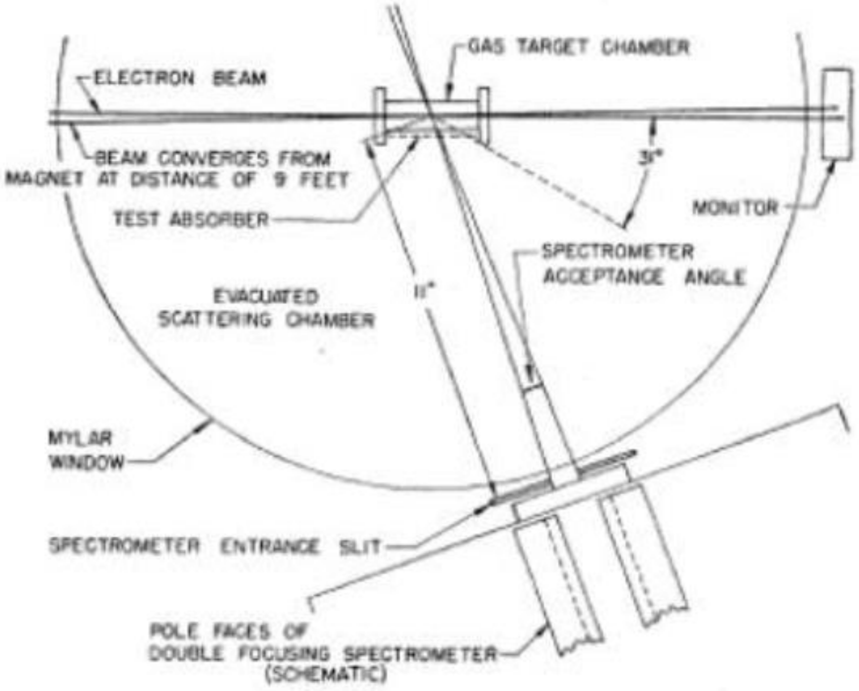

FIG. 2. Arrangement of parts in experiments on electron scattering from a gas target.

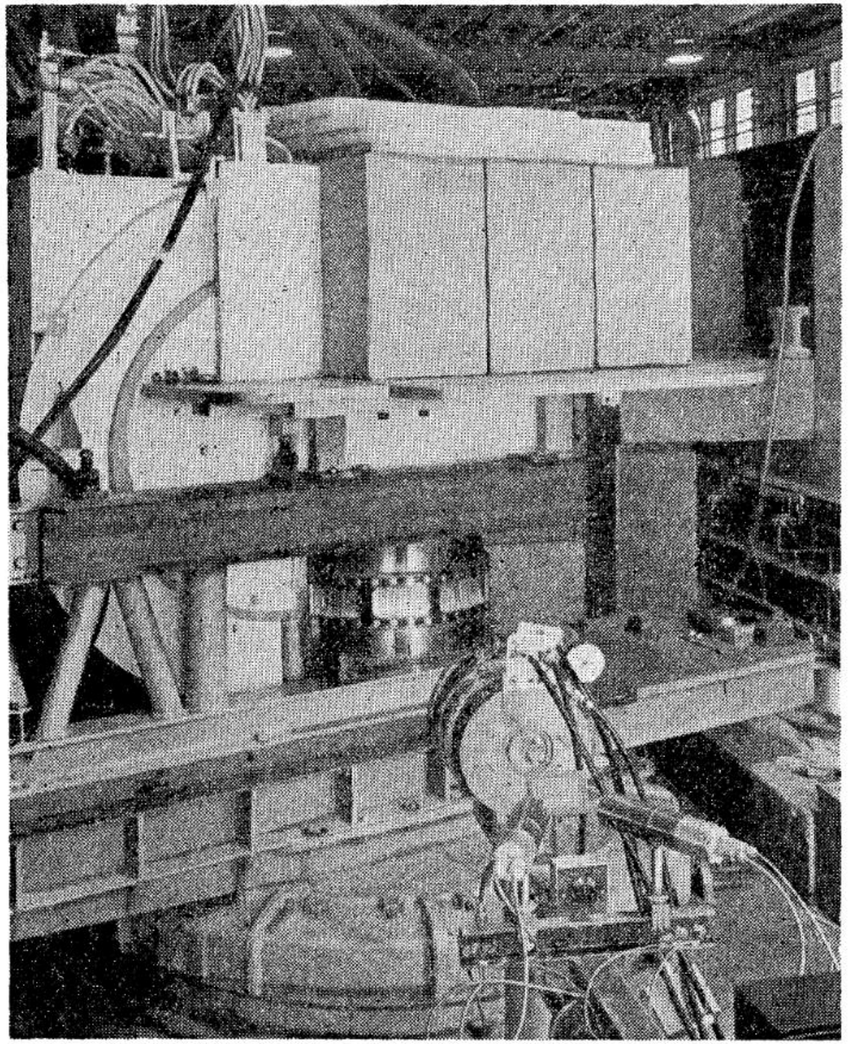

FIG. 15. The semicircular 190-Mev spectrometer, to the left, is shown on the gun mount. The upper platform carries the lead and paraffin shielding that encloses the Čerenkov counter. The brass scattring chamber is shown below with the thin window encircling it. Ion chamber monitors appear in the foreground.

Followed by electron facilities
at Darmstadt, Mainz, Tohoku, Kharkov,
MIT-Bates, ALS Saclay, MAMI and **today JLab 12 GeV 100% duty cycle**

1954-58 at Stanford electron scattering by Hofstadter

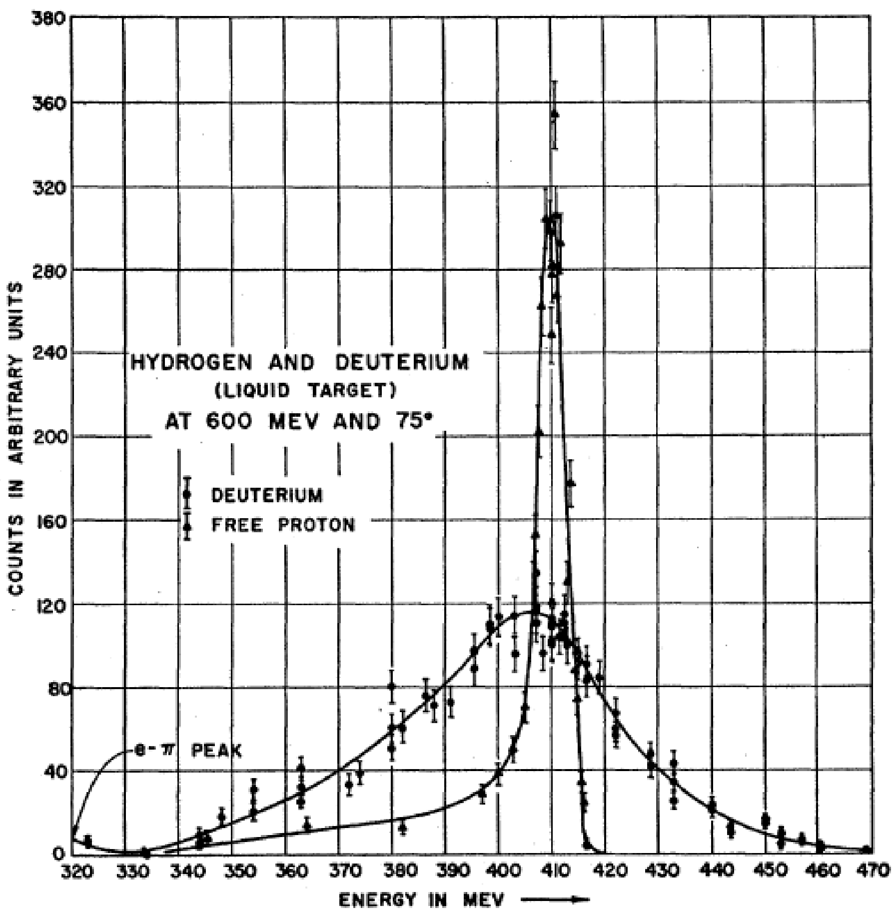

FIG. 19. The inelastic electron-deuteron scattering peak observed at the highest energy (600 Mev) at which such experiments have been carried out. The deuteron curve should be multiplied by 0.87 as in Fig. 17. The data are those of Yearian and Hofstadter[29] and were obtained at a scattering angle of 75° in the laboratory system. The comparison electron-proton peak is also shown in the figure. A point magnetic moment in the neutron would give a larger deuteron scattering peak.

From Hofstadter *et al.*, Review of Modern Physics, Vol 30, 1958

Measurement of the energy spectrum of the scattered electron
for a fixed angle
and a given electron beam energy

H2: peak at the proton kinematic
with the resolution of the spectrometer
+ radiative tail

D2 allows to probe quasi-free proton and neutron
The energy spectrum of the free particle is smeared by the Fermi motion

$$\left(\frac{d\sigma}{d\Omega}\right)_D = \left(\frac{d\sigma}{d\Omega}\right)_P + \left(\frac{d\sigma}{d\Omega}\right)_N$$

1954-58 at Stanford electron scattering by Hofstadter

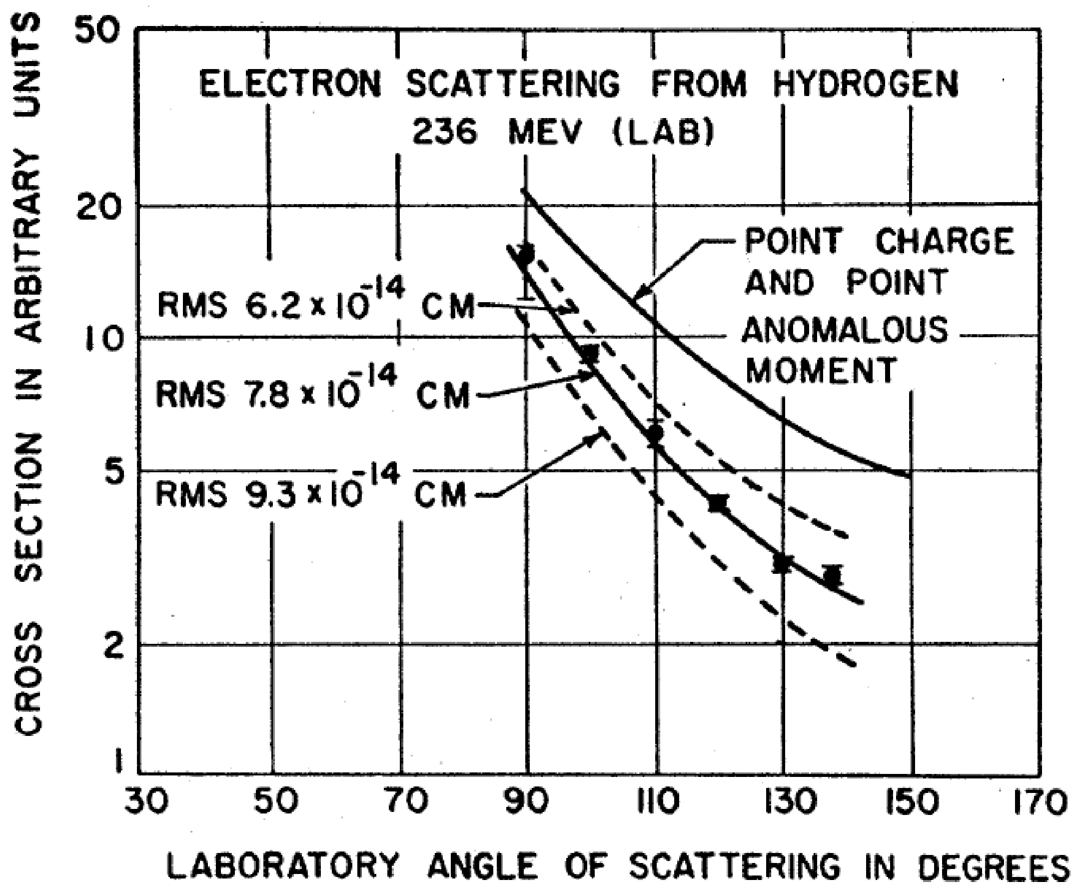

FIG. 3. Experimental points taken at an incident electron energy of 236 Mev are shown. The point-charge, point-moment curve is shown for comparison along with theoretical curves allowing for finite size effects. An rms of 0.78×10^{-13} cm gives good agreement with the experimental data.

From Hofstadter *et al.*, Review of Modern Physics, Vol 30, 1958

$$F_1=F_2 \qquad F=1-(q^2a^2/6)+\cdots, \qquad (6)$$

where "a" is the rms radius of the charge or magnetic moment distribution. Equation (6) can be used where the higher terms in the expansion can be neglected, as in the case of the early data. F is related more generally to a density distribution through the Fourier transform[1,8,9]

The error in the size determination is probably of the order of, or less than, 0.15×10^{-13} cm.

Today 2022 it exists still a fight between

$r^P = 0.84 \pm \sim0.007$ fm

$r^P = 0.88 \pm \sim0.008$ fm

Results for the proton Form Factors (Q^2)

If the proton does not recoil, $M \rightarrow \propto$ and $Q^2 << M^2$, G_E and G_M are the Fourier Transforms of the nucleon charge and magnetization distributions respectively

before 1970

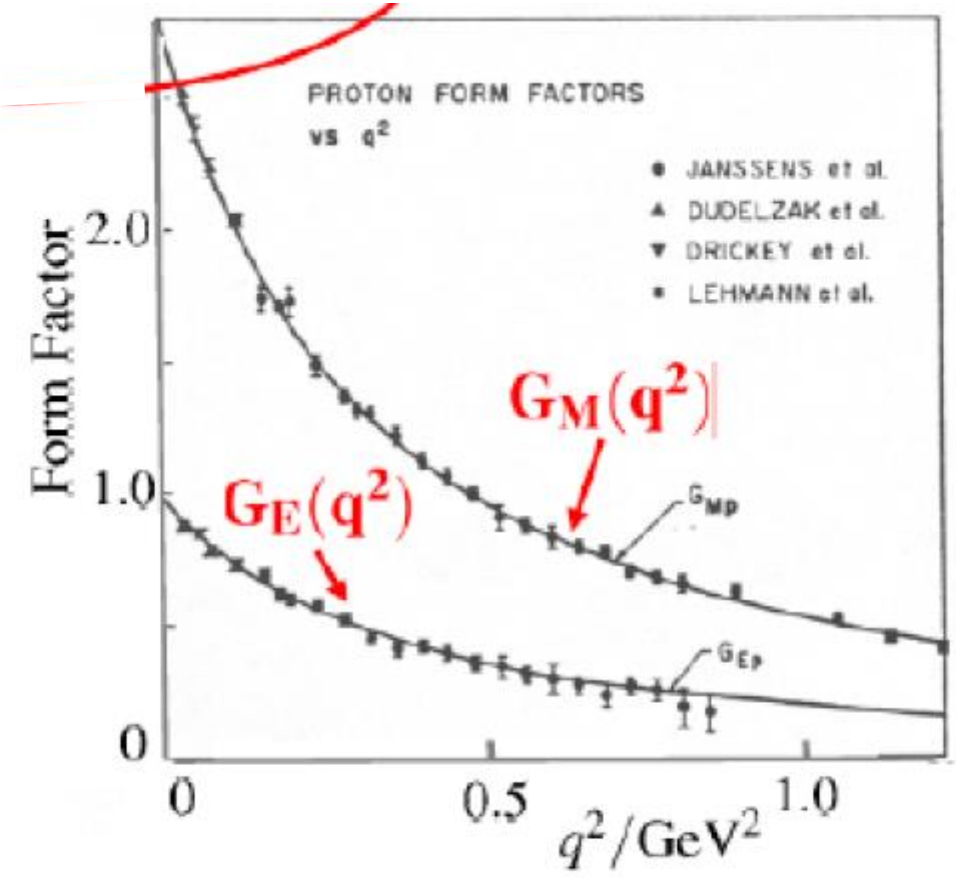

Dipolar Form Factors

$$G_{Ep} = G_D, \; G_{Mp} = \mu_p G_D, \; \text{and} \; G_{Mn} = \mu_n G_D$$

$$G_D = \frac{1}{(1 + Q^2/0.71 GeV^2)^2}$$

The Dipole Form Factor can be interpretated as the Fourier Transform of an exponential distribution
of the proton charge and magnetization density

$G_D = (1 + Q^2 / M_v^2)^{-2}$ $\quad M_v^2 = (0.84 GeV)^2 = 0.71 GeV^2$

$\rho(R) = \rho \exp(-M_V R)$ $\quad R_{rms} = \sqrt{12}/M_V = 0.80$ fm

Results for the proton Form Factors (Q^2)

by Rosenbluth separation

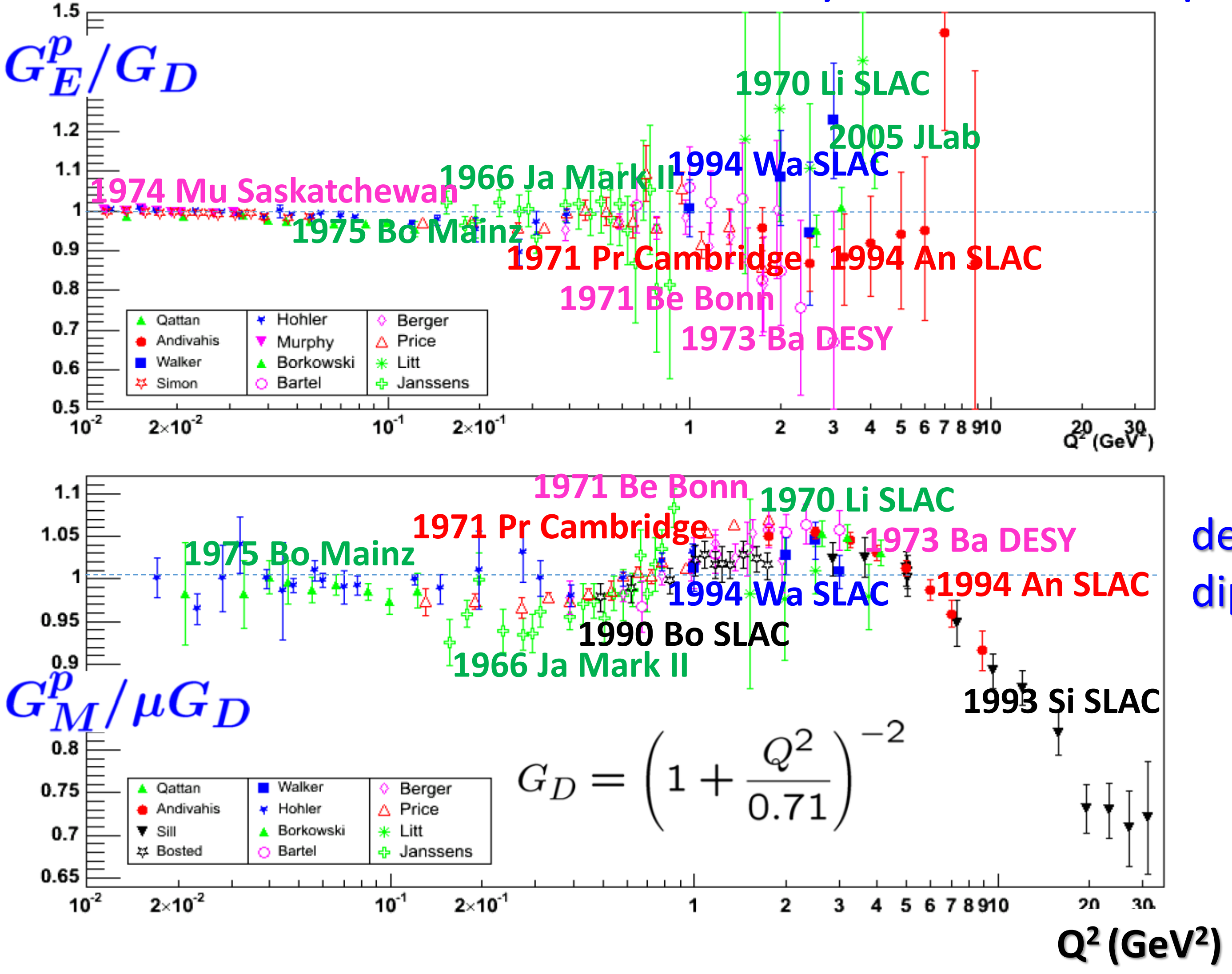

deviation from the dipolar approximation

Results for the proton Form Factors (Q^2)

by double polarization technique

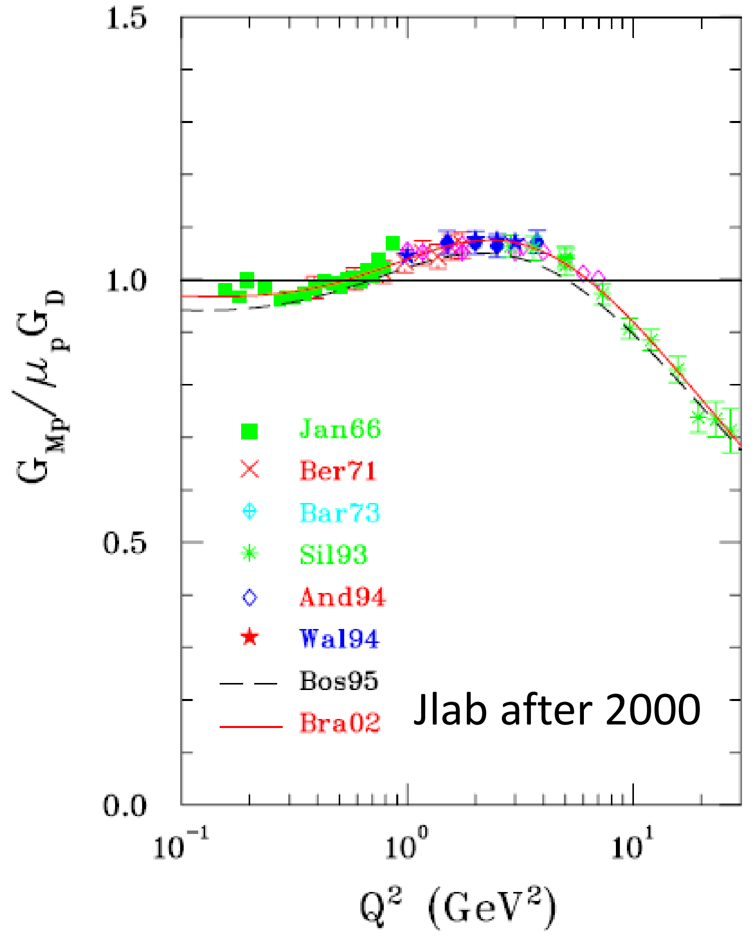

Figure 23: The G_{Mp} data were refitted in [Bra02] imposing the value of the G_{Ep}/G_{Mp} from the recoil polarization data of Refs. [Pun05, Gay02], leaving out Rosenbluth separation data above 1 GeV^2.

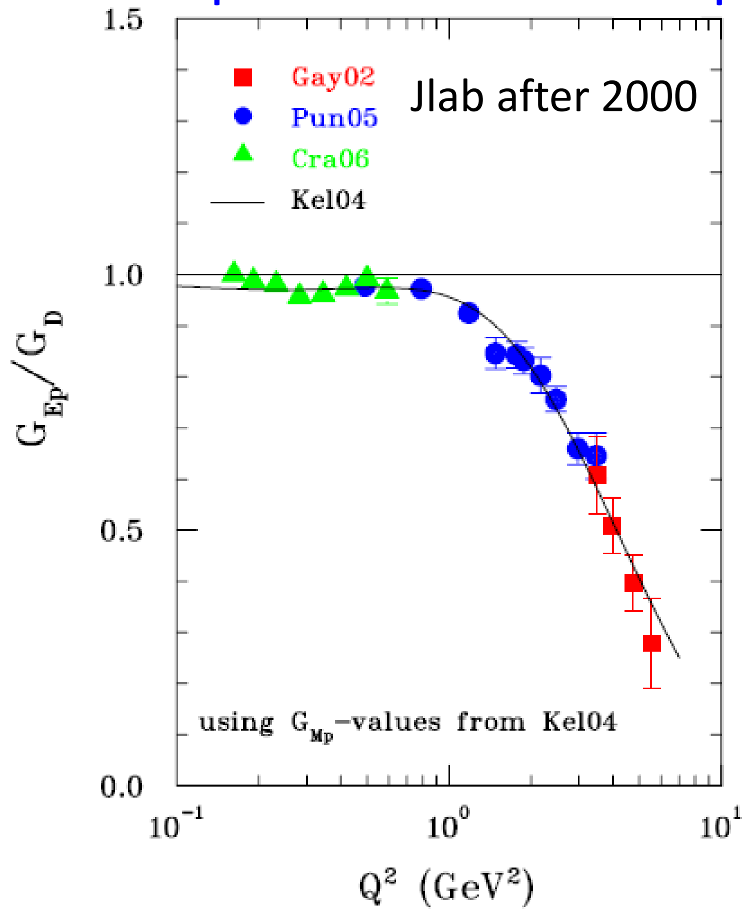

Figure 22: Polarization data presented as G_{Ep}/G_D, where G_{Ep} is obtained from the ratio G_{Ep}/G_{Mp} obtained from polarization data in [Pun05, Gay02, Cra06], multiplied by G_{Mp} from the Kelly fit [Kel04].

G_{Ep} crossing 0 at Q^2= 7 GeV^2?

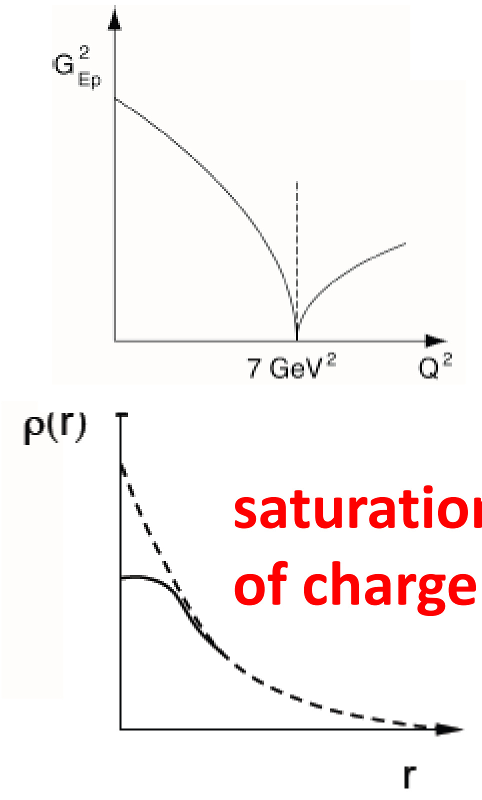

saturation of charge density

A brief story of the particle discovery

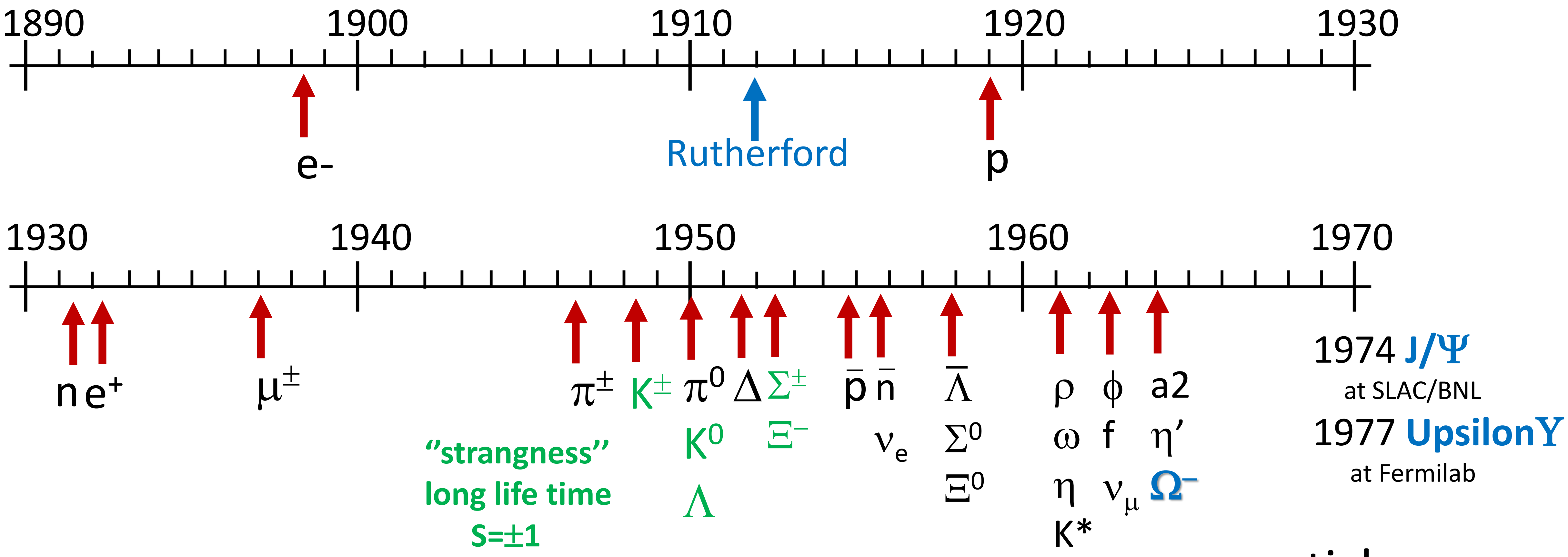

With the advent of accelerators particle zoo

1953 3GeV (1960 33 GeV AGS) BNL@Brookhaven, 1954 7 GeV LBNL@Berckeley, 1959 25 GeV PS (1976 450 GeV SPS) @CERN

1967 tevatron p pbar collider @Fermilab …… 2009 LHC at CERN p p collision 7 TeV against 7 TeV

and Stanford with electron beam 1955 MARKII up to 600 MeV 1962 SLAC up to 60 GeV …

Can all these particles be fundamental?

1960's : Introduction of fractionally-charged quarks

A schematic model of baryons and mesons - Building hadrons from quarks - done independently by Murray Gell-Mann (NP in 69) and George Zweig

In the 1960s, the **first quark models** of elementary particle physics were proposed, which said that protons, neutrons and all other baryons and also all mesons, are made from **three kinds of fractionally-charged particles, the "quarks",** that come in three different types or **"flavors"**, called **up, down, and strange**. ➔ **SU(3) group**

The quark was hypothesized to be a building block in the sense that individual quarks do not exist in isolation but bind with antiquarks or pairs of quarks to form **$q\bar{q}$ states for mesons** and **qqq states for baryons.**

	u	d	s
Charge	2/3	-1/3	-1/3
I3	1/2	-1/2	0
S	0	0	-1

.

First Meson nonets (8 ⊕ 1) in SU(3)

$J^{PC} = 0^{-+}$ Pseudoscalar meson

$J^{PC} = 1^{--}$ Vector meson

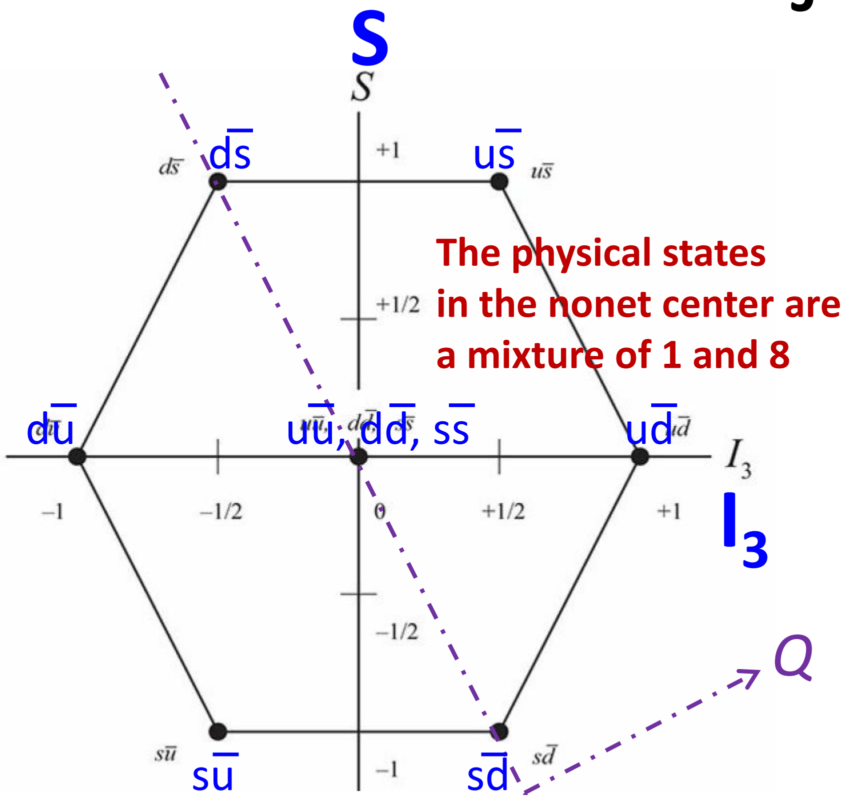

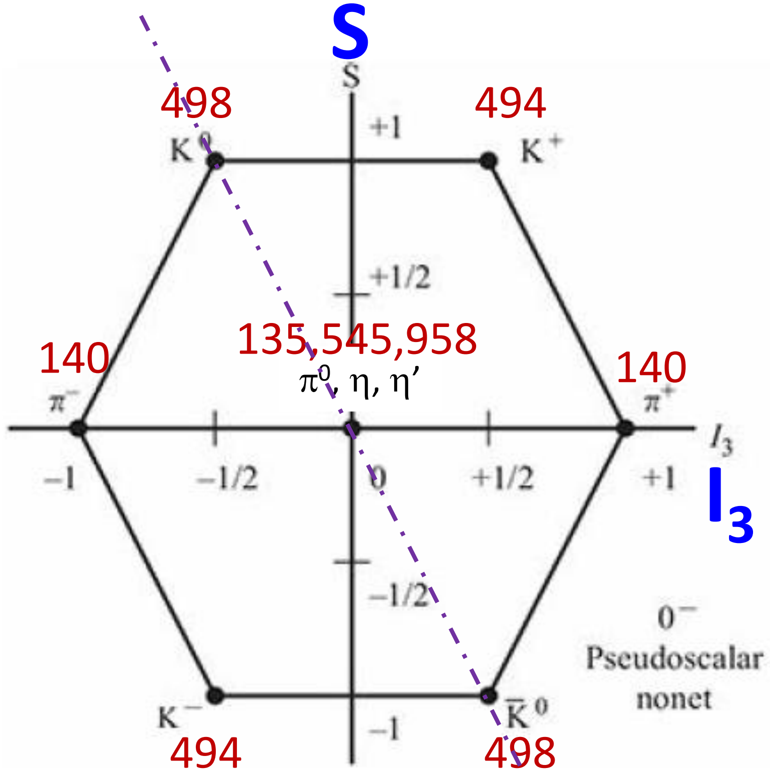

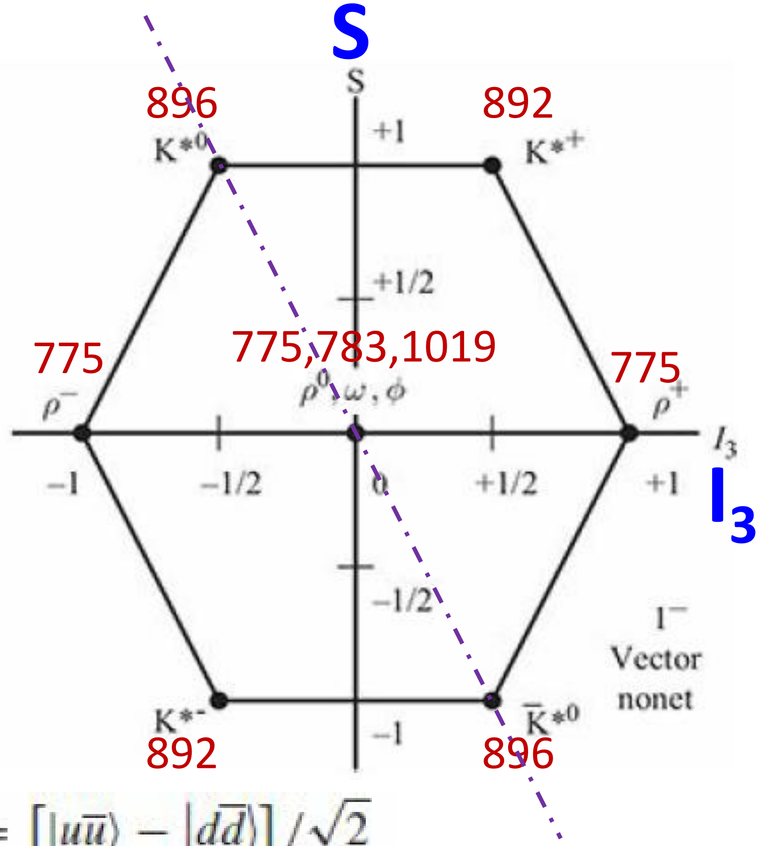

$|1;0,0\rangle = [|u\bar{u}\rangle + |d\bar{d}\rangle + |s\bar{s}\rangle]/\sqrt{3} \equiv \phi_1 \equiv \eta_1$

$|8;1,0\rangle = [|u\bar{u}\rangle - |d\bar{d}\rangle]/\sqrt{2}$

$|8;0,0\rangle = [|u\bar{u}\rangle + |d\bar{d}\rangle - 2|s\bar{s}\rangle]/\sqrt{6} \equiv \phi_8 \equiv \eta_8$

$|N;I,I_3\rangle$

$\pi^0 = [|u\bar{u}\rangle - |d\bar{d}\rangle]/\sqrt{2}$ ↔ $\rho^0 = [|u\bar{u}\rangle - |d\bar{d}\rangle]/\sqrt{2}$

$$\begin{pmatrix} \cos\theta_P & -\sin\theta_P \\ \sin\theta_P & \cos\theta_P \end{pmatrix} \begin{pmatrix} \eta_8 \\ \eta_1 \end{pmatrix} = \begin{pmatrix} \eta \\ \eta' \end{pmatrix}$$

$\omega = [|u\bar{u}\rangle + |d\bar{d}\rangle]/\sqrt{2} = \sqrt{2/3}\phi_1 + \sqrt{1/3}\phi_8$

$\phi = |s\bar{s}\rangle = \sqrt{1/3}\phi_1 - \sqrt{2/3}\phi_8$

In theory θ_p *=35°; exp* θ_p *~11° for η η'*

Baryon singlet, octet and decuplet in SU(3)

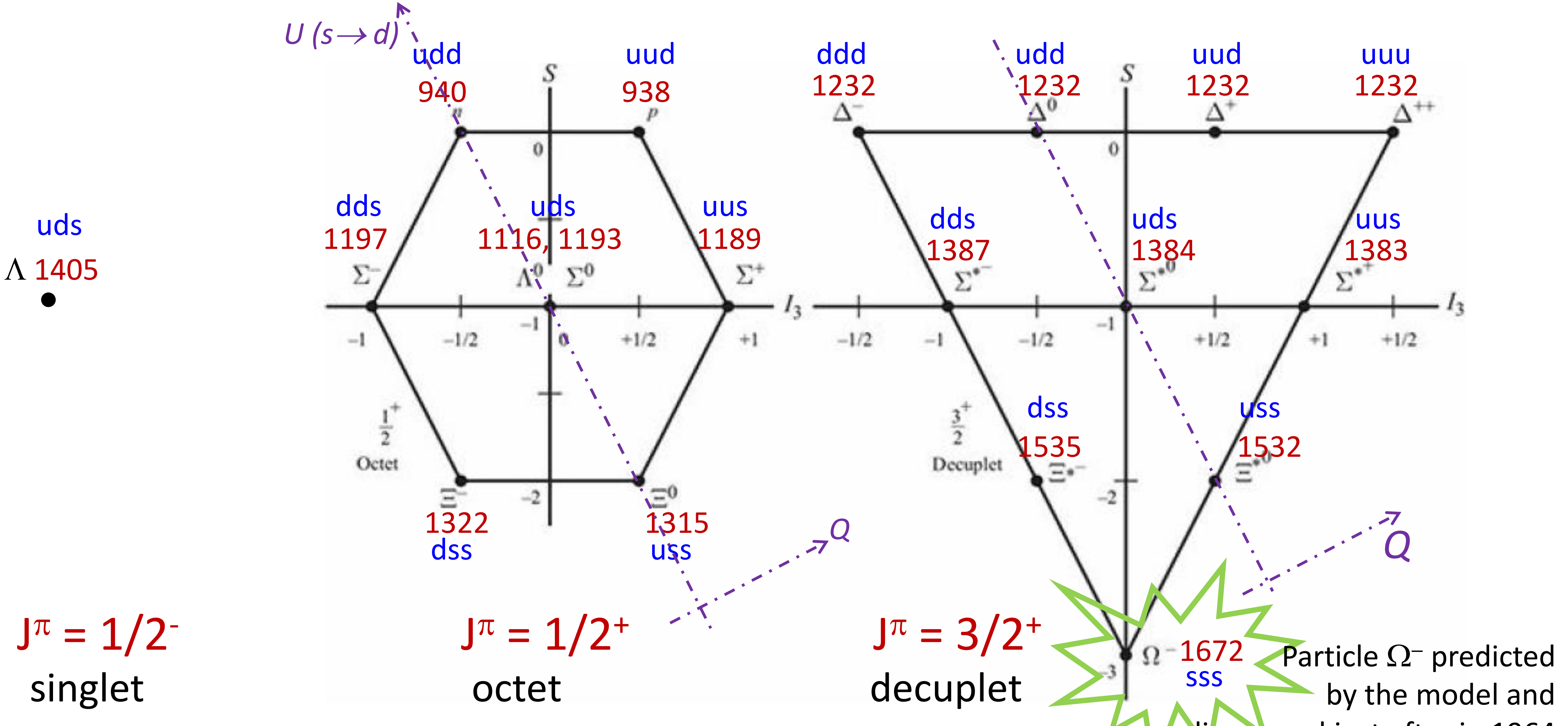

Mass splittings due to SU(3) symmetry breaking ($m_s \neq m_d \cong m_d$)

SUCCES of the SU(3) but why octet $J^{\pi} = 1/2^{+}$...?

Hypothetic quarks to real current quarks

Murray Gell-Mann (NP in 69) and George Zweig

1964: the quark lodel

- The model had one serious problem....
  The free quarks were not observed in the nature...
- "To many physicists this was not surprising. Fractional charges were considered to be a really strange and unacceptable concept, and the general point of view in 1966 was that quarks were most likely just mathematical representations - useful but not real".

Quotation from a Nobel price winner J. J. Friedman

1968: deep inelastic scattering experiments conducted by Friedmann, Kendall and Taylor (PN in 90) with electron beams at SLAC revealed surprising experimental evidence for particles inside of protons. To a first approximation, they were indeed the already-described quarks.

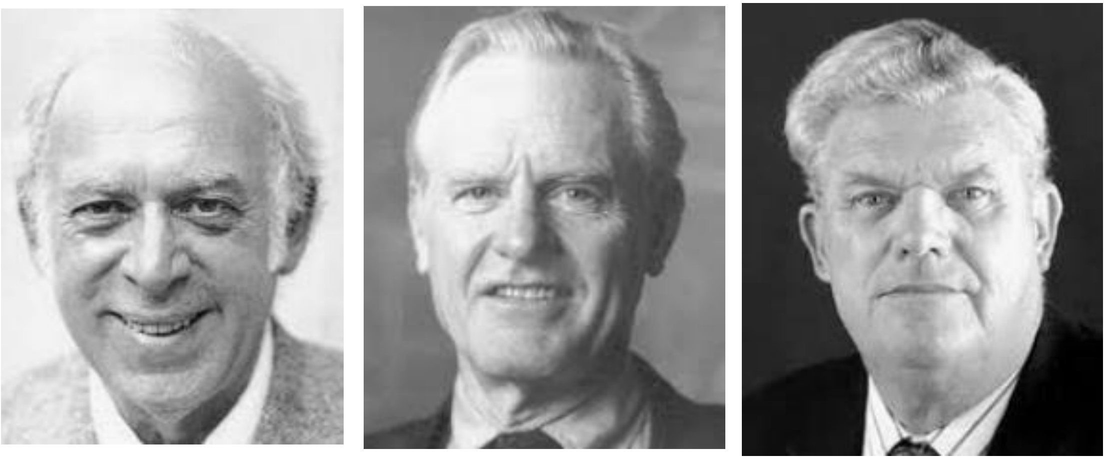

Friedmann, Kendall (MIT) and Taylor (SLAC) (NP in 90)

Probing: Lepton-nucleon scattering

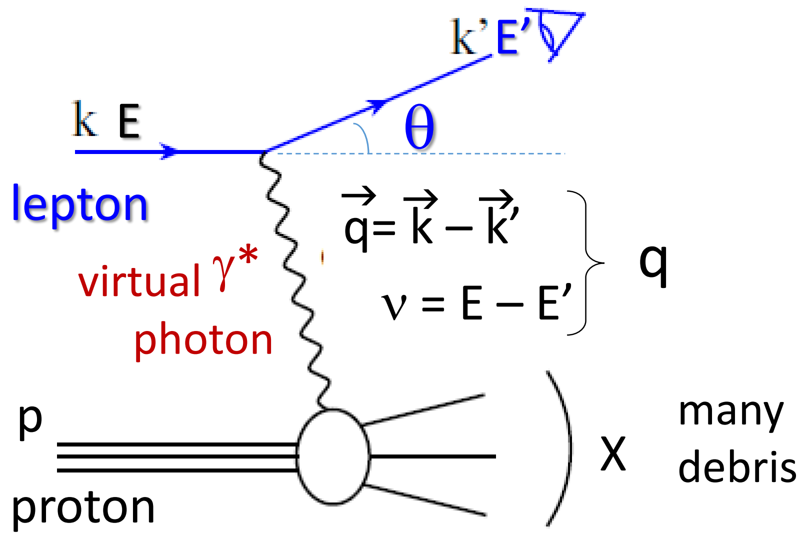

Hypotheses:

- ✓One photon exchanged
- ✓M_{e-} <<

in lab.

$Q^2 = -q^2 \quad = 4\,E\,E'\sin^2\theta/2 > 0$

for fixed target

$x_B = Q^2/(2p.q) = Q^2/(2M_p\nu)$

Elastic Scattering: e p → e' p' X=proton

at fixed beam energy E, only one other variable, Q^2 or θ (or E')

$(p+q)^2 = W^2 = M_p^2 - Q^2 + 2p.q = M_p^2 \Rightarrow \quad x_B = 1$

Deep Inelastic Scattering (DIS): the proton is broken in many debris X

$(p+q)^2 = W^2 = M_p^2 - Q^2 + 2p.q > M_p^2 \quad \Rightarrow \quad 0 < x_B < 1$

at fixed beam energy E, 2 variables (E', θ) or (Q^2, x_B) or (Q^2, ν)

Q^2 and ν varie independently

$\Delta x = \hbar c/\sqrt{Q^2}$ spatial resolution

$\Delta t = \hbar c/\nu$ time resolution

Observation of the 2 cross sections: elastic and DIS

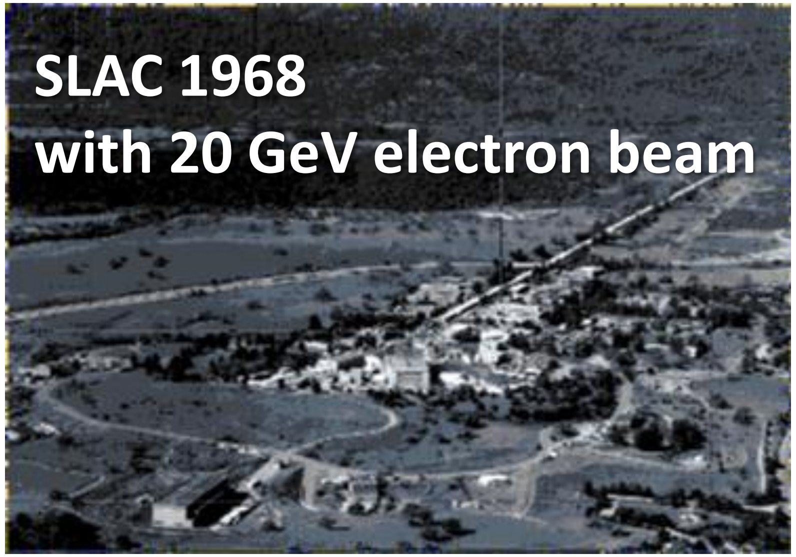

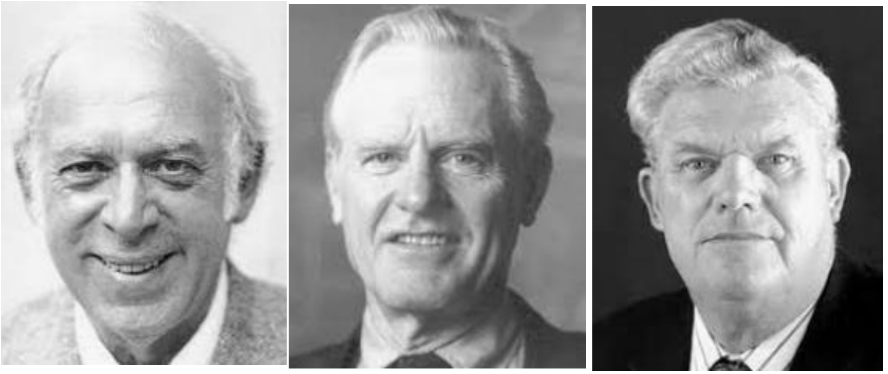

Friedmann, Kendall (MIT)
and Taylor (SLAC)
(Nobel Prices in 1990)

M.Breidenbach et al.,
Phys. Rev. Lett. 23 (1969) 935

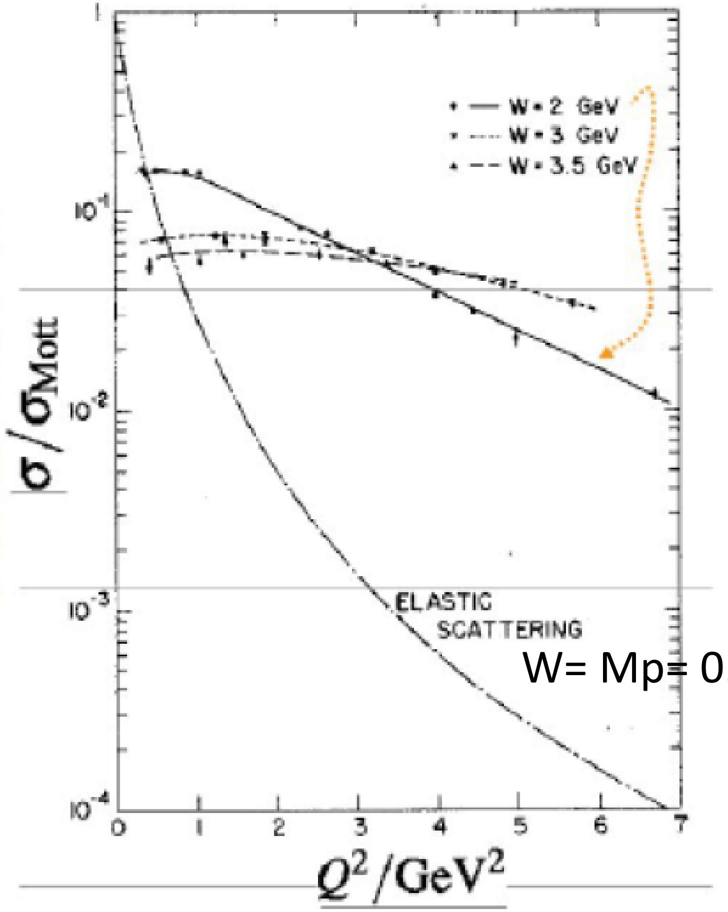

In 1968, it was a great surprise, when for the first time, the SLAC-MIT experiments showed that at large Q^2, the DIS cross sections appeared much larger than expected. The DIS cross Section is almost constant while the elastic one drops 3 orders of magnitude.

much larger than expected? ….similar to the Rutherford experiment??

This suggests that some sort of violent collisions with point-like objects is underlying dynamical mechanism at work

DIS cross section and observation of the scaling

$$\left(\frac{d^2\sigma}{d\Omega dE'}\right)_{lab} = \sigma_{Mott}\left[W_2(\nu, Q^2) + W_1(\nu, Q^2)\tan^2(\theta/2)\right]$$

James Bjorken, theoretician at SLAC

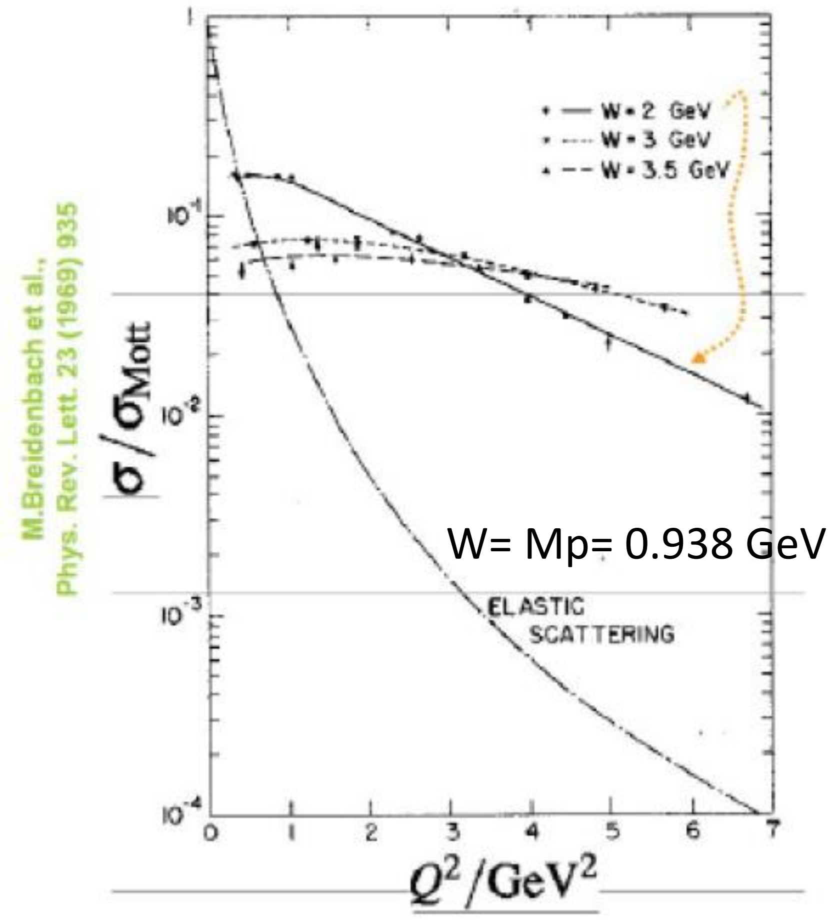

$$\text{if } W \nearrow \qquad M_p W_1(\nu, Q^2) \xrightarrow{\nu, Q^2 \to \infty} F_1(x_B)$$
$$\nu W_2(\nu, Q^2) \longrightarrow F_2(x_B)$$

scaling

$$\text{if } W = M_p \qquad M_p W_1(\nu, Q^2) \xrightarrow{\nu, Q^2 \to \infty} 0$$
$$\nu W_2(\nu, Q^2) \longrightarrow 0$$

Understanding of the scaling → hypothesis of quarks

if $W \nearrow$

$$M_p W_1(\nu, Q^2) \xrightarrow{\nu, Q^2 \to \infty} F_1(x_B)$$
$$\nu W_2(\nu, Q^2) \longrightarrow F_2(x_B)$$

- υW_2 and W_1 independent of Q^2
- υW_2 and $W_1 \nearrow$ when $x_B \searrow$

Panofsky, director of SLAC in 1968, presenting these results at the Wien Conference: ''… Therefore, theoretial speculations are focused on the possibility that these data might give evidence on the behaviour of point-like, charged structures within the nucleon.''

Fig. 12.11. Scaling behaviour of electromagnetic structure function νW_2 at various ω values. There is virtually no variation with Q^2. (From Panofsky, 1968.)

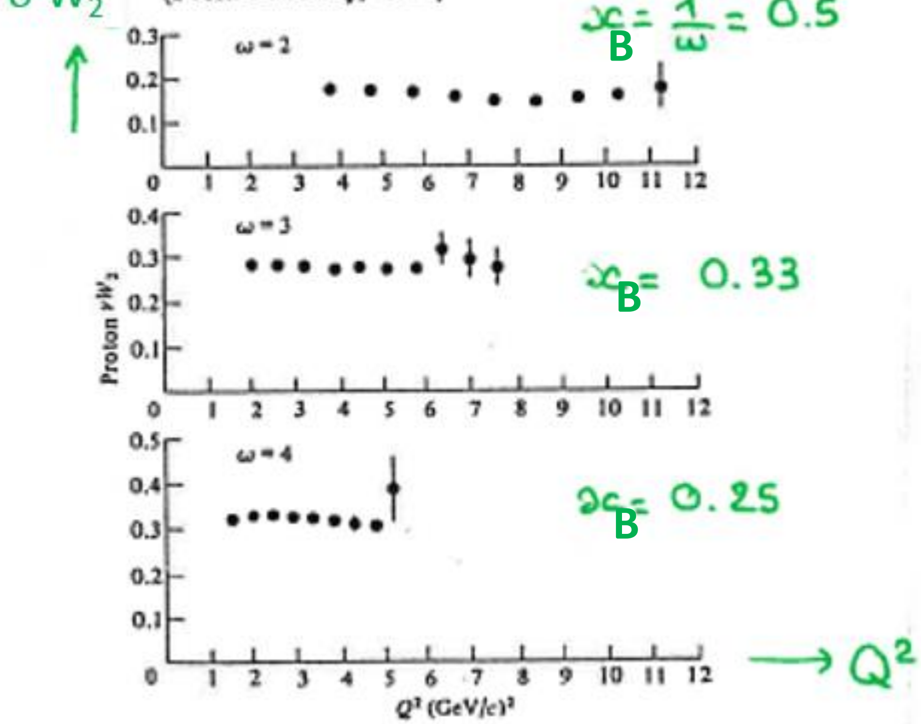

Fig. 12.12. Scaling behaviour of electromagnetic structure function $2m_N W_1$. Almost no Q^2 dependence is visible. (From Panofsky, 1968.)

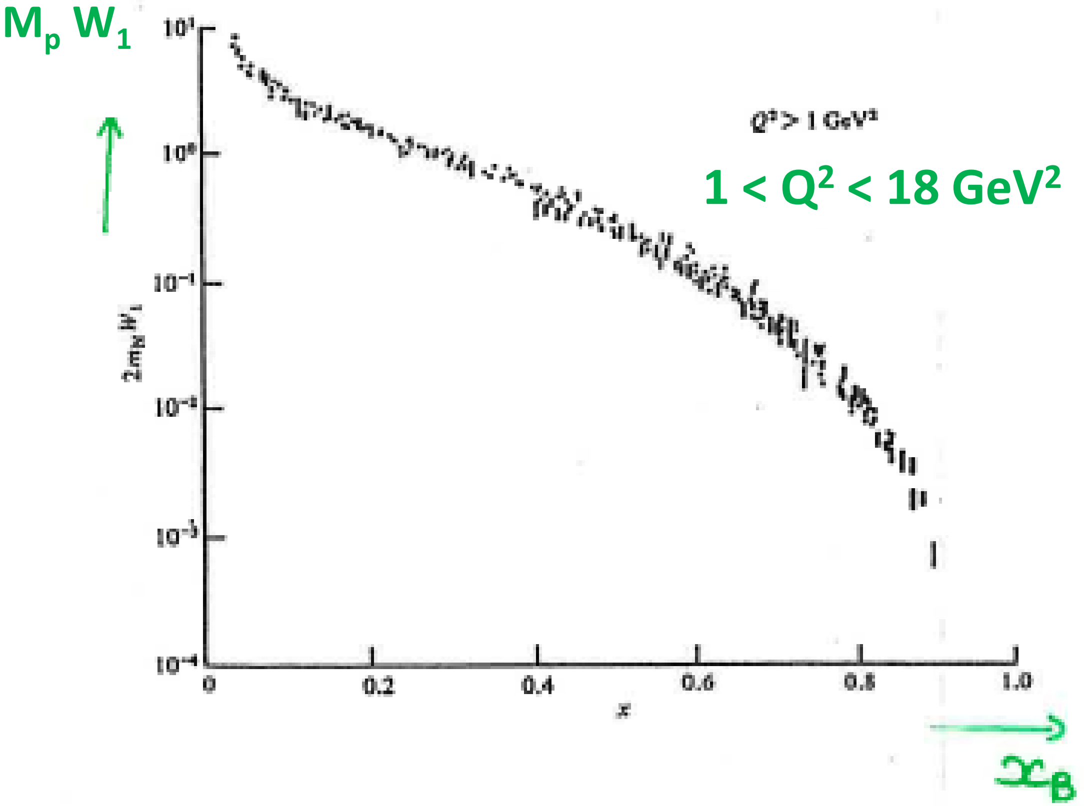

Interpretation in the Quark Parton Model

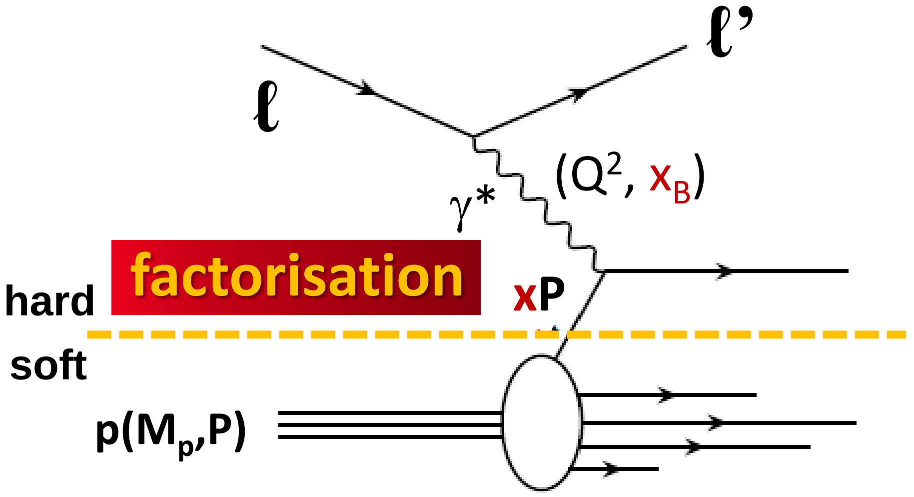

time $_{\gamma^* q \text{ interaction}}$ << time $_{\text{hadronization}}$

free partons confined partons

Quark Parton Model (QPM) from Richard Feynman 1969:

In the frame of the collision γ^* p at very large energy ➔ Lorentz boost

- longitudinal size contracted
- time dilatation

➢ Point-like, non-interacting partons (free partons in a large jail)

➢ Collinear to the nucleon movement (P >> M_p) in photon-nucleon collision (longitudinal direction)

➢ Each parton carries a fraction x of the nucleon momentum

➢ The struck parton verifies: **$x = x_B$**

Deep Inelastic Scattering (DIS):

factorisation

$$\sigma_{DIS}(ep \rightarrow e X) = \sum_{q,x}^{\text{incoherent}} \sigma_{elastic}(eq \rightarrow eq) \otimes q(x)$$

Parton Distribution Function q(x) =

Probability to find a parton q of longitudinal momentum fraction x

Scaling q(x) but violation $q(x,Q^2)$

Universality of the PDF to describe the nucleon structure

Application of the Quark Parton Model

$$F_2(x) = x \sum_q e_q^2 \, q(x)$$

$$F_1(x) = \frac{1}{2} \sum_q e_q^2 \, q(x)$$

$$F_2(x) = 2 \, x \, F_1(x)$$

Callan-Gross relation - The partons are of spin ½

The partons are identified to the quarks introduced for the hadron spectrum

Application of the Quark Parton Model

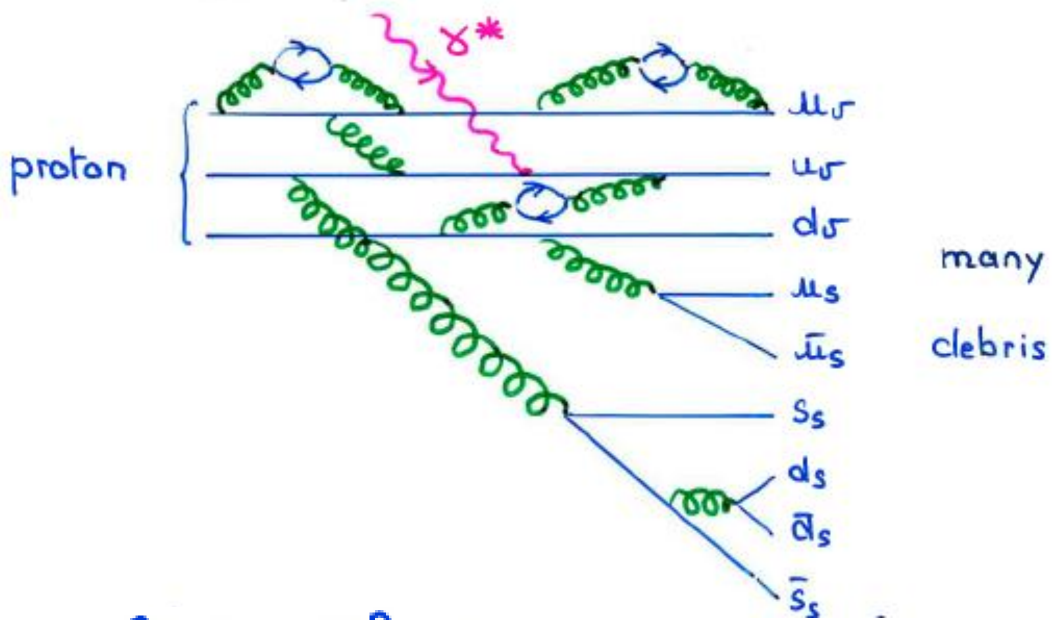

$u^p(x)$, $\bar{u}^p(x)$

probability distributions of u quarks and antiquarks in the proton

(p, n) isospin doublet

$$\begin{cases} u^p(x) = d^n(x) = u(x) \\ d^p(x) = u^n(x) = d(x) \\ s^p(x) = s^n(x) = s(x) \end{cases}$$

electromagnetic structure fonction $F_2(x)$

proton = $u_v u_v d_v$ + many $q\bar{q}$ pairs radiated by the valence quarks ⇝ we assume the 3 lighest flavor quarks (u, d, s) to occur in the "sea" with roughly the same frequency and momentum distribution (heavier flavor q pairs are neglected)

$$\begin{cases} u(x) = u_v(x) + u_s(x) \\ d(x) = d_v(x) + d_s(x) \\ u_s(x) = \bar{u}_s(x) = d_s(x) = \bar{d}_s(x) = s_s(x) = \bar{s}_s(x) = S(x) \end{cases}$$

$$\frac{1}{x} F_2^{ep}(x) = \left(\frac{2}{3}\right)^2 [u^p(x) + \bar{u}^p(x)] + \left(\frac{1}{3}\right)^2 [d^p(x) + \bar{d}^p(x)] + \left(\frac{1}{3}\right)^2 [s^p(x) + \bar{s}^p(x)]$$

$$\frac{1}{x} F_2^{ep}(x) = \frac{4}{9} u_v(x) + \frac{1}{9} d_v(x) + \frac{12}{9} S(x)$$

$$\frac{1}{x} F_2^{en}(x) = \frac{1}{9} u_v(x) + \frac{4}{9} d_v(x) + \frac{12}{9} S(x)$$

Where are the gluons?

momentum conservation $$\sum_q \int_0^1 dx\, x\, q(x) = 1$$

$$\int_0^1 dx\, x\, (u(x)+\bar{u}(x)+d(x)+\bar{d}(x)+s(x)+\bar{s}(x)) = 1-\varepsilon_g$$

ε_g fraction of momentum carried by the gluons

$$\varepsilon_u \equiv \int_0^1 dx\, x\, (u(x)+\bar{u}(x))$$
$$\varepsilon_d \equiv \int_0^1 dx\, x\, (d(x)+\bar{d}(x))$$
$$\varepsilon_s \equiv \int_0^1 dx\, x\, (s(x)+\bar{s}(x)) = 0 \text{ (assumpt.)}$$

we measure
$$\int dx\, F_2^{ep}(x) = \frac{4}{9}\varepsilon_u + \frac{1}{9}\varepsilon_d = 0.18$$
$$\int dx\, F_2^{em}(x) = \frac{1}{9}\varepsilon_u + \frac{4}{9}\varepsilon_d = 0.12$$

$\Rightarrow$ $\varepsilon_u = 0.36$ $\varepsilon_d = 0.18$ $\varepsilon_g = 0.46$

the gluons carry about 50% of the momentum, which was not accounted by the charged quarks

the momentum distribution of the quarks forces us to the conclusion that a substantial fraction of the proton's momentum is carried by neutral partons. These are the gluons of QCD.

Limit of the scaling

Limit : Scaling violation

how does the gluon bremsstrahlung contribute to the structure functions?

if $x \leq 0.2$ $F_2(x Q^2) \nearrow$ when $Q^2 \nearrow$
if $x \geq 0.2$ $F_2(x Q^2) \searrow$ when $Q^2 \nearrow$

$F_2(x Q^2)$ shifts its $\langle x \rangle$ from large to small values as $Q^2 \nearrow$
because the high resolution photons have more chance of seeing "softer" quarks whose momentum has been degrated by gluon emission

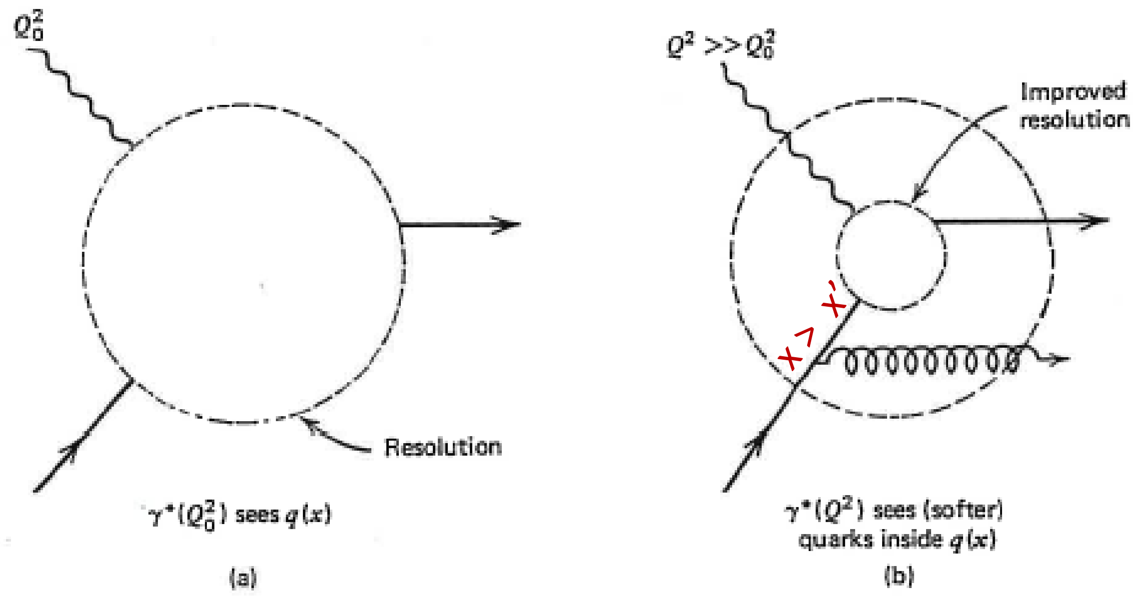

Fig. 10.9 The quark structure of the proton as seen by a virtual photon as Q^2 increases.

équation dite "DGLAP" pour Dokshitzer, Gribov, Lipatov, Altarelli, Parisi.

$$\frac{d}{d\log Q^2}\begin{pmatrix} q(x,Q^2) \\ g(x,Q^2) \end{pmatrix} = \frac{\alpha_s}{2\pi}\begin{pmatrix} P_{qq} & P_{qg} \\ P_{gq} & P_{gg} \end{pmatrix}\begin{pmatrix} q \\ g \end{pmatrix}$$

Summary of the Structure Function F_2

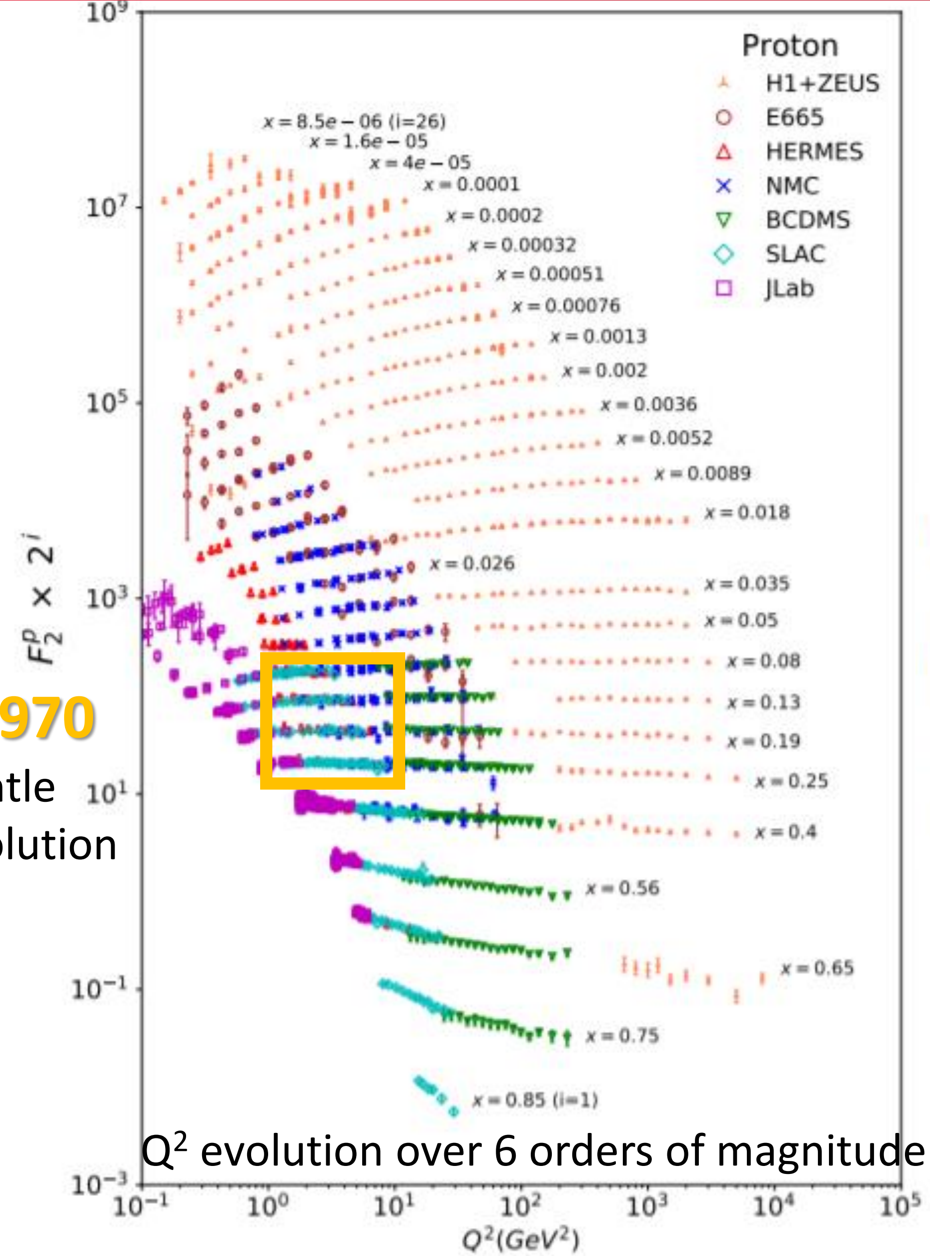

SLAC1970

Very gentle QCD evolution

TODAY 50 years after PDG 2020

Figure 18.8: The proton structure function F_2^p measured in electromagnetic scattering of electrons and positrons on protons, and for electrons/positrons (SLAC,HERMES,JLAB) and muons (BCDMS, E665, NMC) on a fixed target. Statistical and systematic errors added in quadrature are shown. The H1+ZEUS combined values are obtained from the measured reduced cross section and converted to F_2^p with a HERA-PDF NLO fit, for all measured points where the predicted ratio of F_2^p to reduced cross-section was within 10% of unity. The data are plotted as a function of Q^2 in bins of fixed x. Some points have been slightly offset in Q^2 for clarity. The H1+ZEUS combined binning in x is used in this plot; all other data are rebinned to the x values of these data. For the purpose of plotting, F_2^p has been multiplied by 2^{i_x}, where i_x is the number of the x bin, ranging from $i_x = 1$ ($x = 0.85$) to $i_x = 26$ ($x = 0.0000085$). Only data with $W^2 > 3.5$ GeV^2 is included. P

In 2020: x from 10^{-5} to 0.85 and Q^2 from 0.1 to 10^5

In 2010: x from $5\ 10^{-4}$ to 0.65 and Q^2 from 1 to 10^5

Unpolarized quark and gluon PDFs

Global fit on the world data

(uncertainties arising from experimental errors and model assumptions

PDG 2020

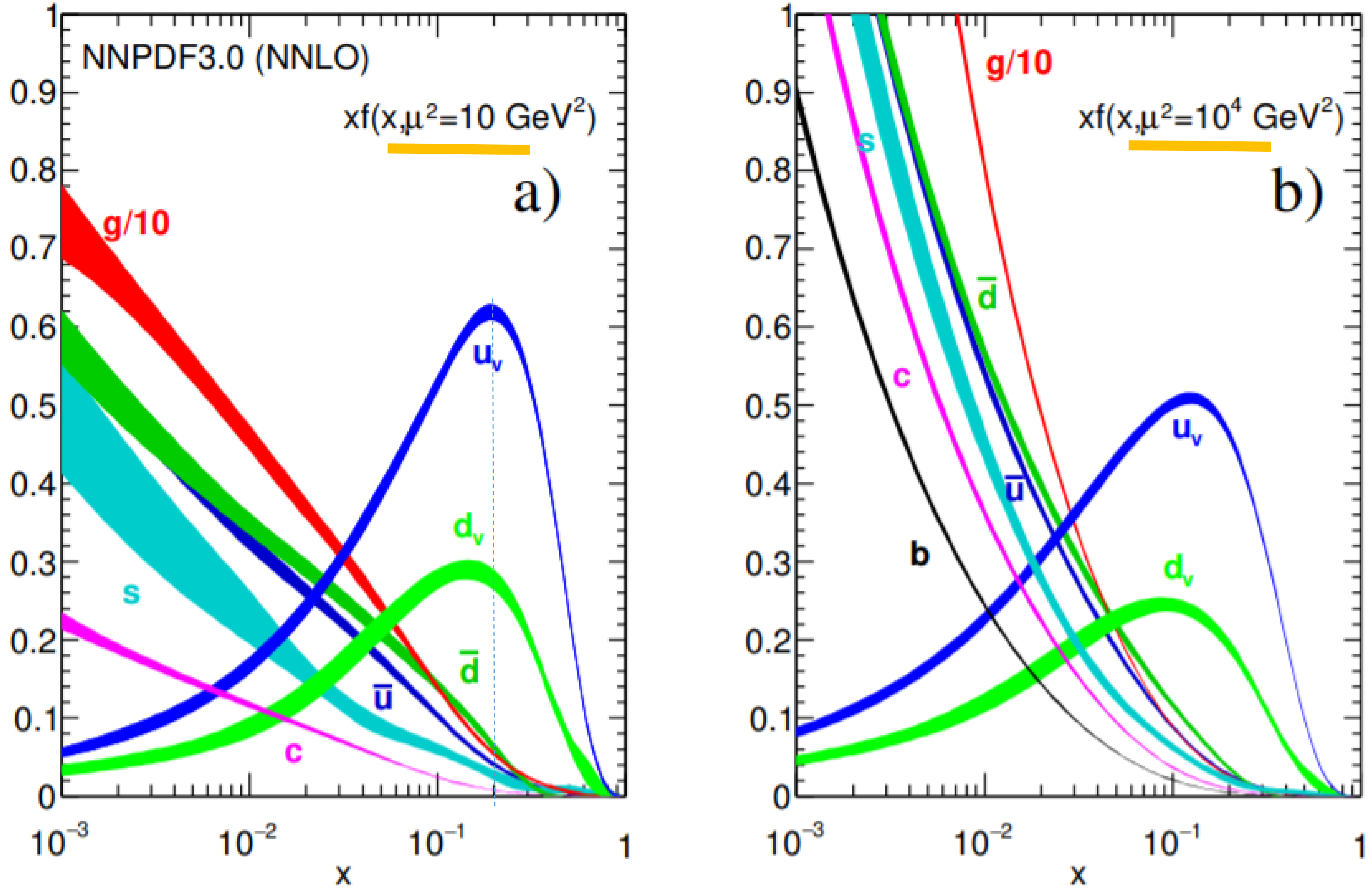

A few main facilities in the world up to now

Tremendous experimental efforts matched by theoretical progress

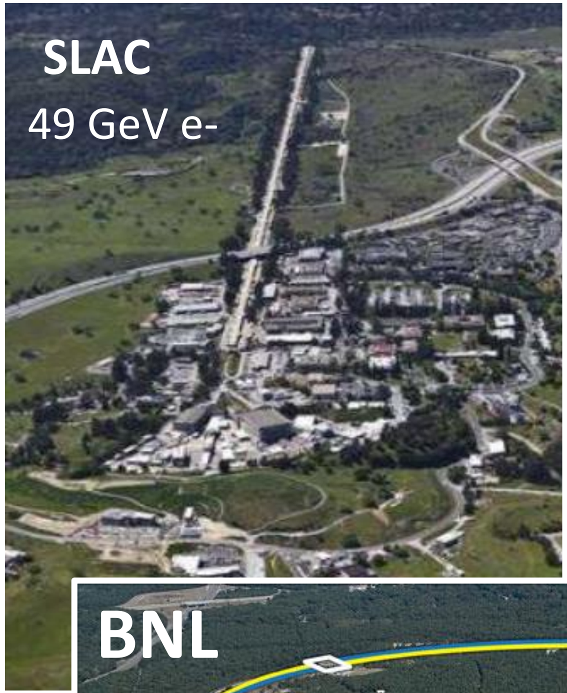

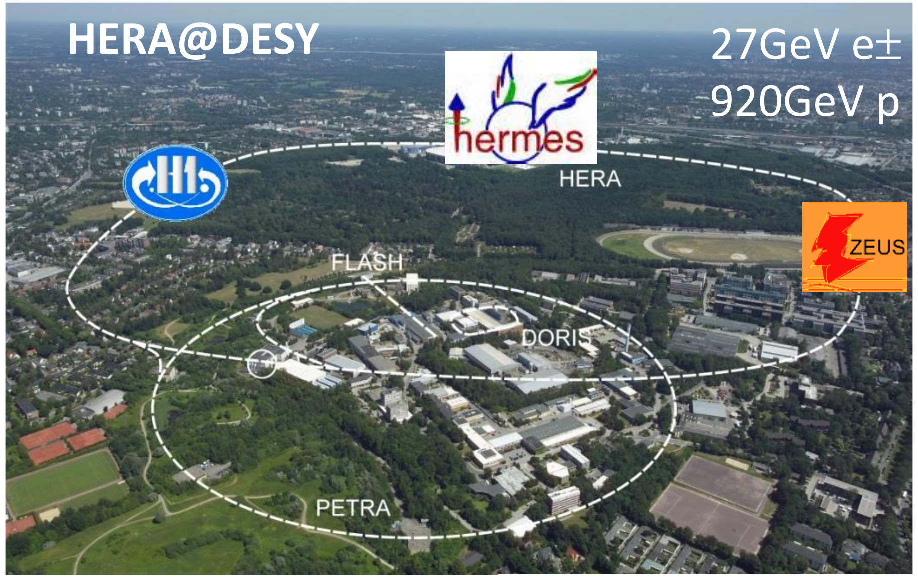

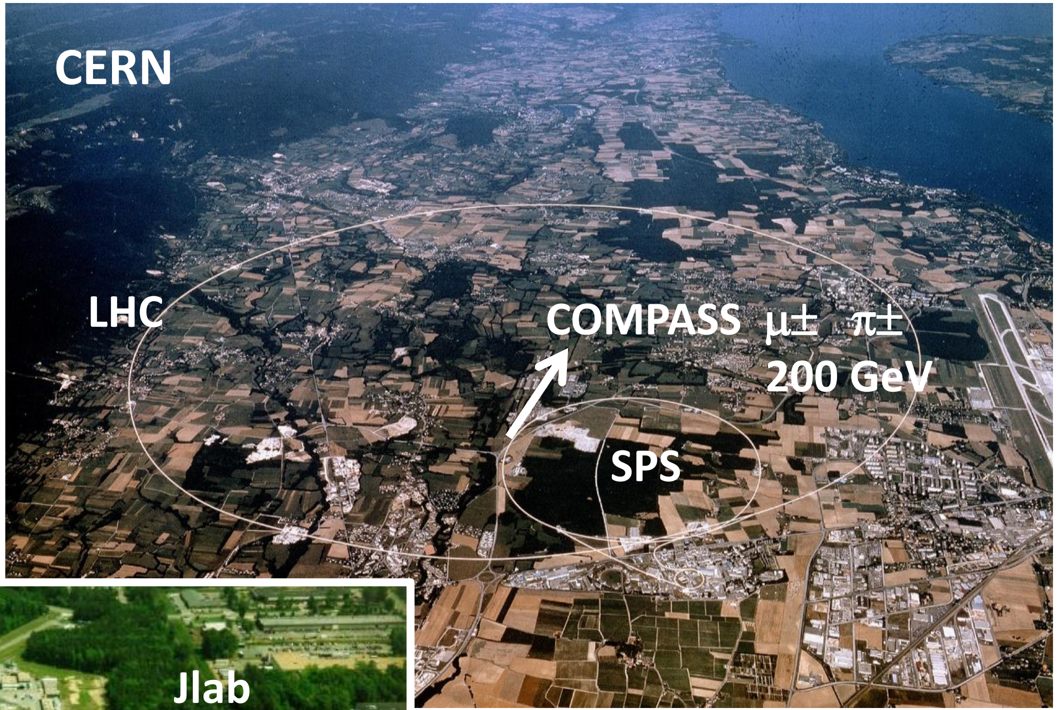

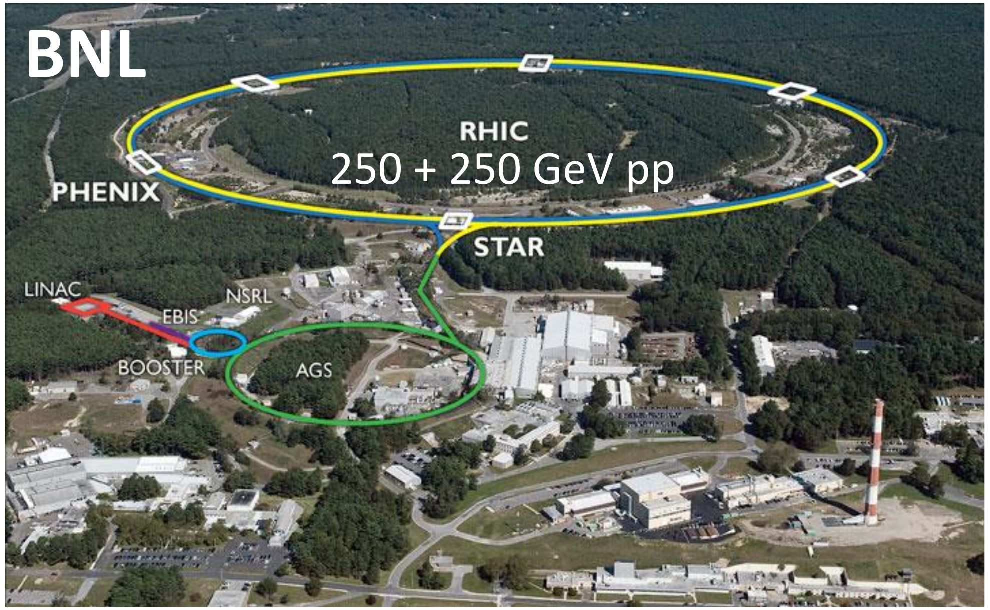

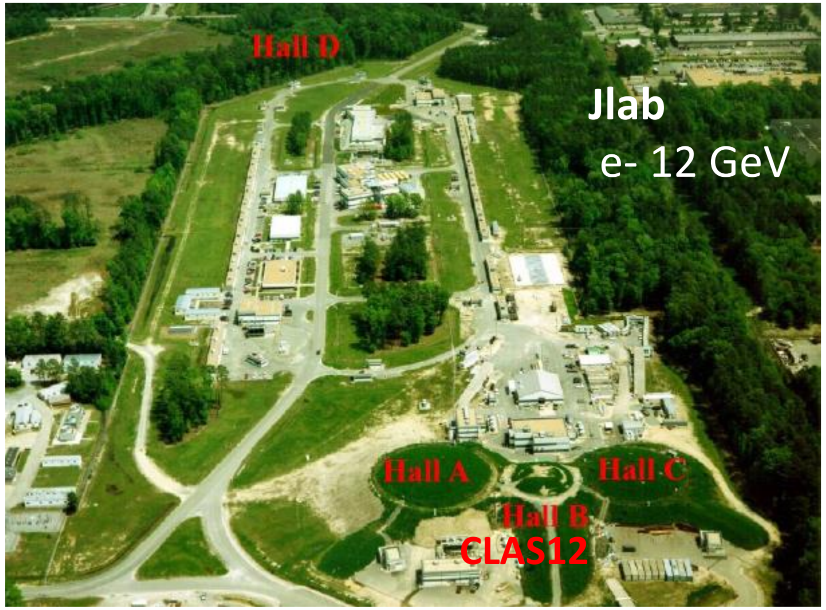

+ KEK 6 GeV $e^+ e^-$ (Belle) + ...

+ EIC (CD0 2019 CD1 2021 → 2032)
up to 275 GeV hadrons on
18 GeV electrons at BNL + ...

Fixed target: $s = 2ME$

Collider: $s = 4E_1E_2$

Confinement not explained by the QPM

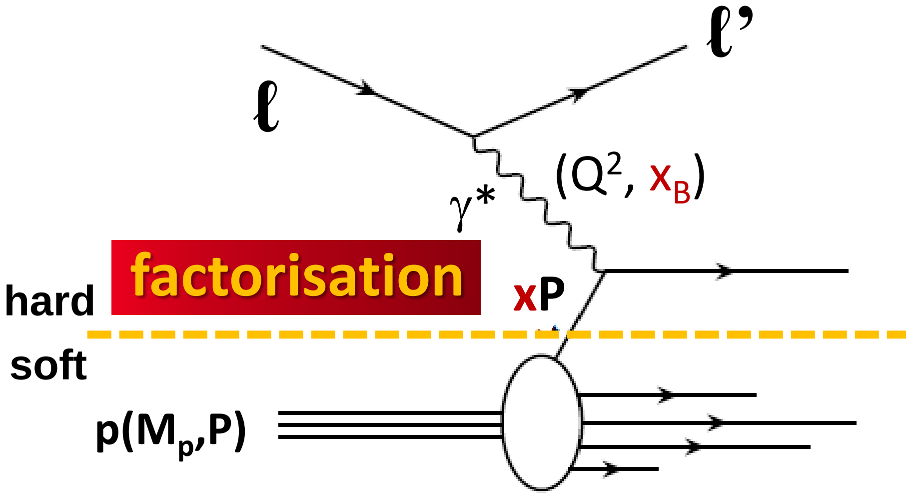

time $_{\gamma^* q \text{ interaction}}$ << time $_{\text{hadronization}}$

free partons confined partons

Quark Parton Model (QPM) from Richard Feynman 1969:

In the frame of the collision γ^* p at very large energy ➔ Lorentz boost
- longitudinal size contracted
- time dilatation

- ➢ Point-like, non-interacting partons (free partons in a large jail)
- ➢ Collinear to the nucleon movement (P >> M_p) in photon-nucleon collision (longitudinal direction)
- ➢ Each parton carries a fraction x of the nucleon momentum
- ➢ The struck parton verifies: **$x = x_B$**

Since the proton is composed of quarks confined by gluons, an equivalent pressure which acts on the quarks can be defined. This allows calculation of their distribution as a function of distance from the centre using an **exclusive reaction as the Compton Scattering of high-energy electrons on the proton.**

Proton picture: from 1D to (1+ 2)D

going to the most complete description of the nucleon

Q^2, x_{Bj}

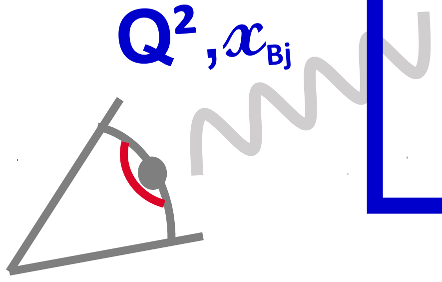

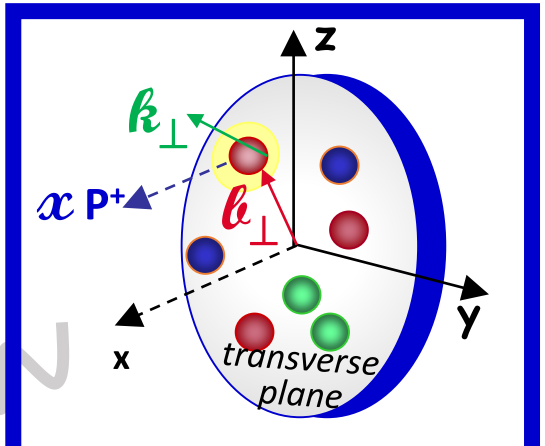

$\mathcal{W}(x, k_\perp, b_\perp)$

Quantum tomography of the nucleon

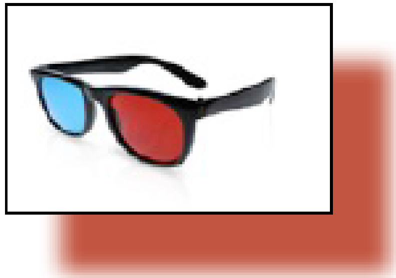

Ji, PRL91 (2003)
Belitsky, Ji, Yuan, PRD69 (2004)
Lorcé et al, JHEP1105 (2011)

$\int db_\perp$ $\int dk_\perp$

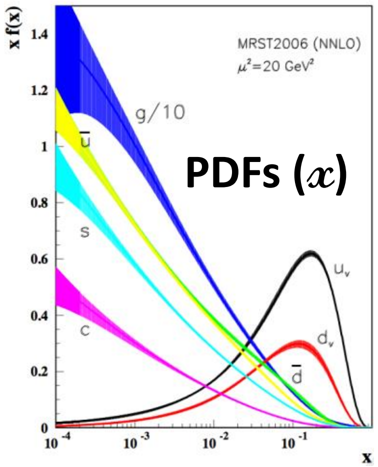

Transverse momentum

f $(x, k_\perp)$
8 TMDs

accessible in SIDIS *and* Drell-Yan

$\int dk_\perp$

Transverse position

q $(x, b_\perp)$
8 GPDs

$\int dx$ → **Form Factors**

$\int db_\perp$

PDFs (x)

accessible in **exclusive reactions**

DVCS: Deeply Virtual Compton Scattering
HEMP: Hard Exclusive Meson Production

Deeply Virtual Compton Scattering

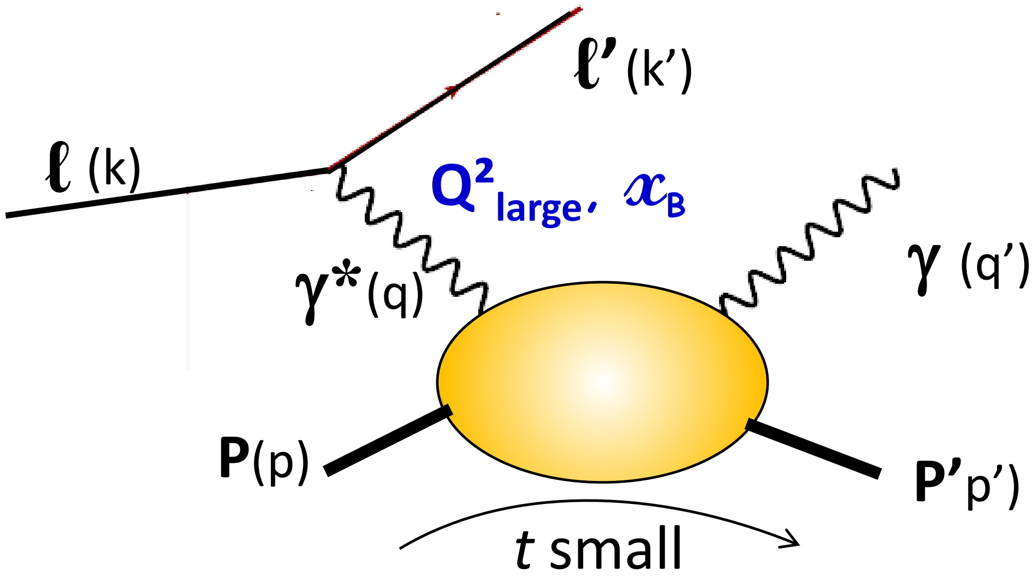

DVCS: $\ell p \rightarrow \ell' p' \gamma$

the golden channel because it interferes with the Bethe-Heitler process (exactly calculable in QED)

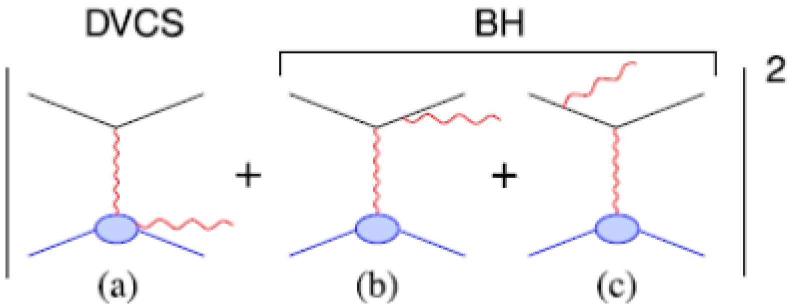

The 5 experimental variables:

- lepton beam (charge, polarisation): E_ℓ , Q^2 >1 GeV^2, x_B
- t = $(p-p')^2$ = $(q-q')^2$ < 1 or a few GeV^2 ($|t|/Q^2 < 0.20$)
- ϕ angle between $\ell\ell'$ plane and $\gamma\gamma^*$ plane

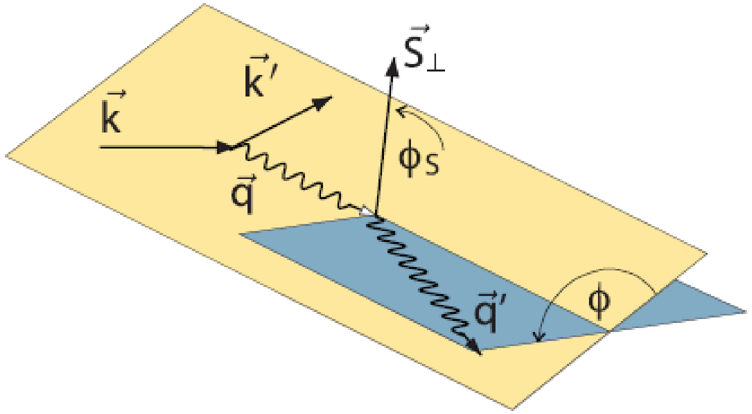

DVCS and BH contributions at COMPASS

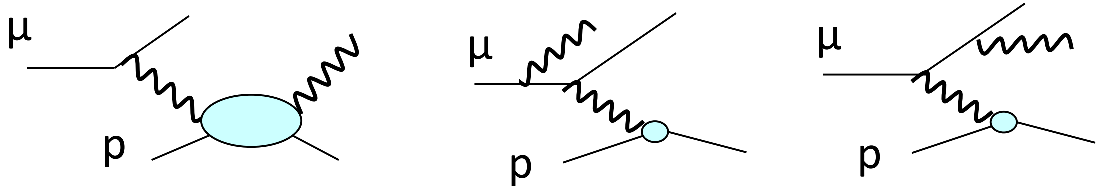

DVCS BH calculable

The high energy muon beam at COMPASS allows to play with the relative contributions DVCS-BH which depend on $1/y = 2\ m_p\ E_\ell\ x_B\ /Q^2$

Higher energy (or higher x_B): DVCS>>BH
➔ DVCS Cross section

Smaller energy (or smaller x_B): DVCS~BH
➔ Interference term and DVCS amplitude

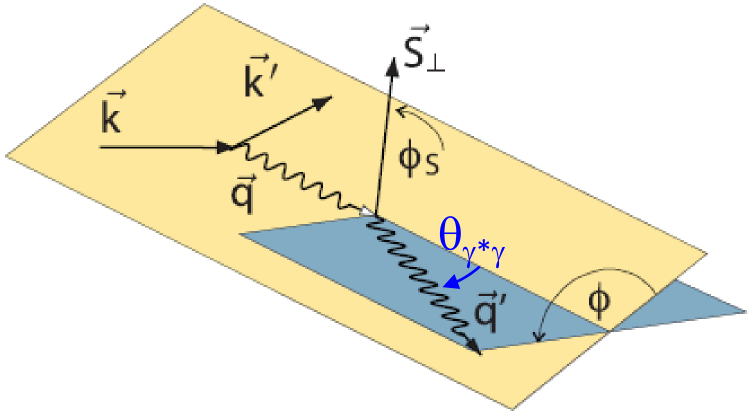

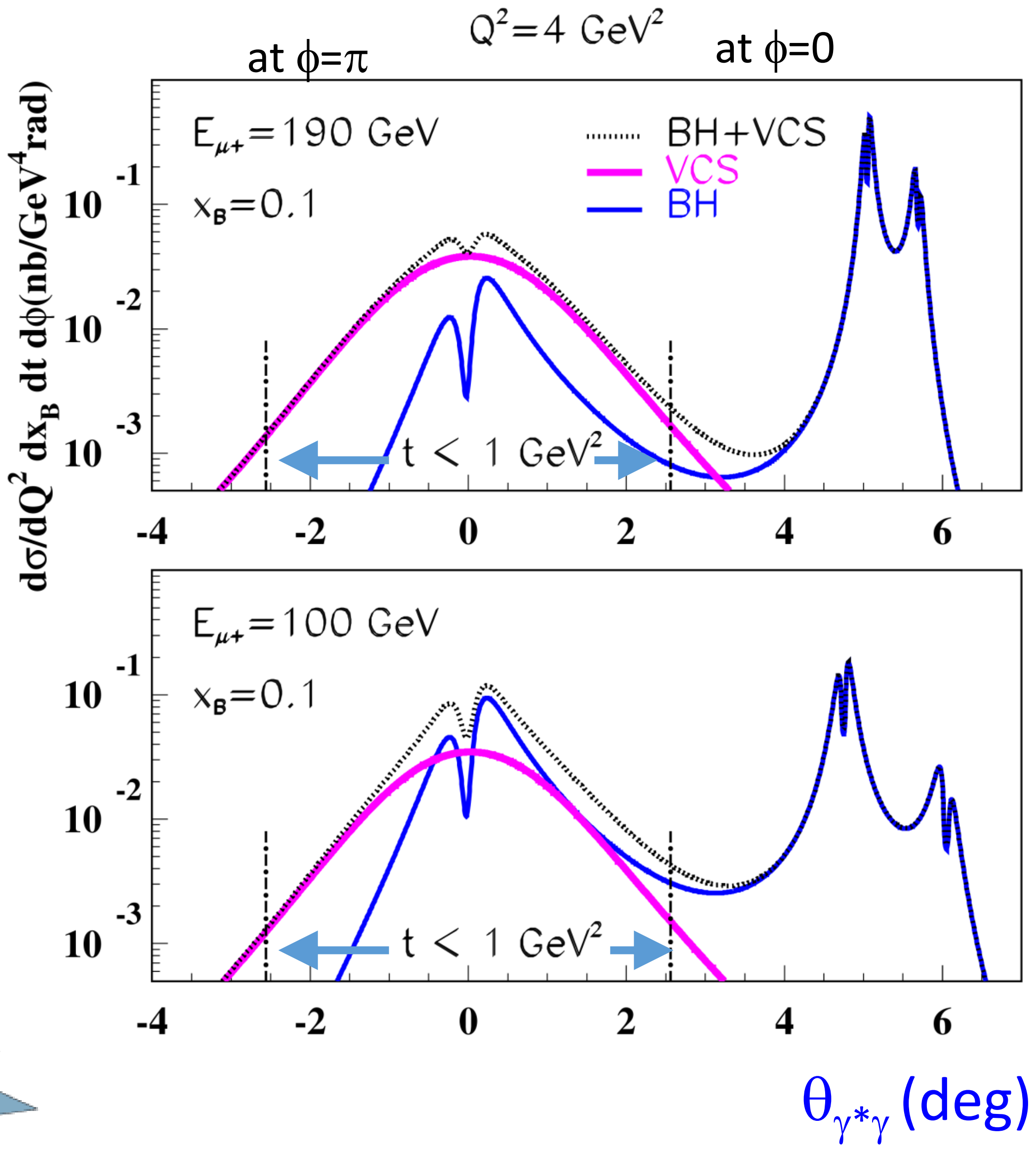

Hard Exclusive Meson Production

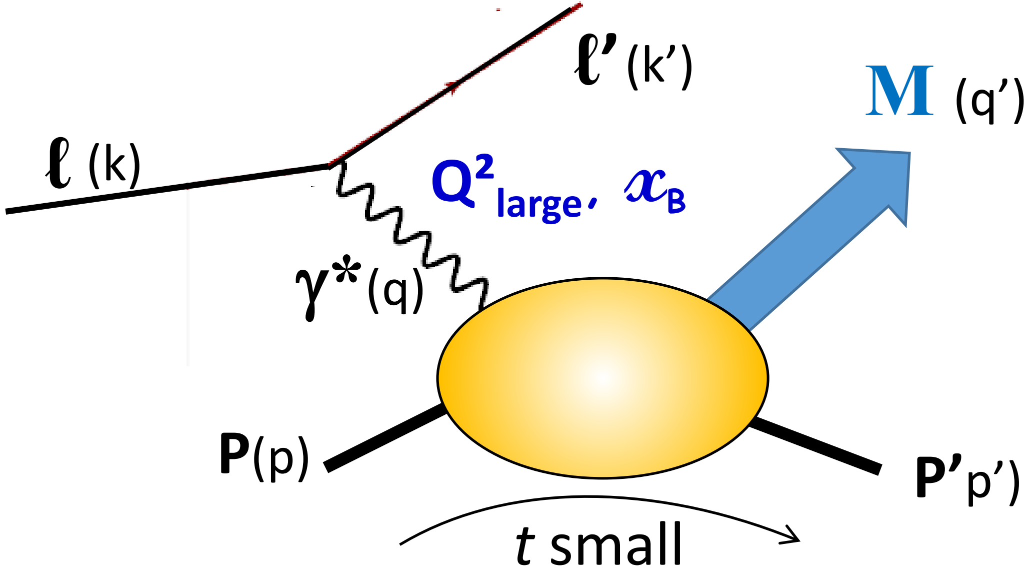

Pseudo-scalar meson π, η …

Vector Meson ρ, ω or ϕ or J/ψ…

G=(-1)^L+S+I

	L	S	I	G
$\pi^0 = [\lvert u\bar{u}\rangle - \lvert d\bar{d}\rangle]/\sqrt{2}$	0	0	1	-
$\eta \approx [\lvert u\bar{u}\rangle + \lvert d\bar{d}\rangle - 2\lvert s\bar{s}\rangle]/\sqrt{6}$	0	0	0	+
$\rho^0 = [\lvert u\bar{u}\rangle - \lvert d\bar{d}\rangle]/\sqrt{2}$	0	1	1	+
$\omega = [\lvert u\bar{u}\rangle + \lvert d\bar{d}\rangle]/\sqrt{2}$	0	1	0	-
$\phi = \lvert s\bar{s}\rangle$	0	1	0	-
J/ψ = |cc>	0	1	0	-

Flavor filter and decomposition

Exclusive reactions have small cross section

At Q^2=0 GeV^2

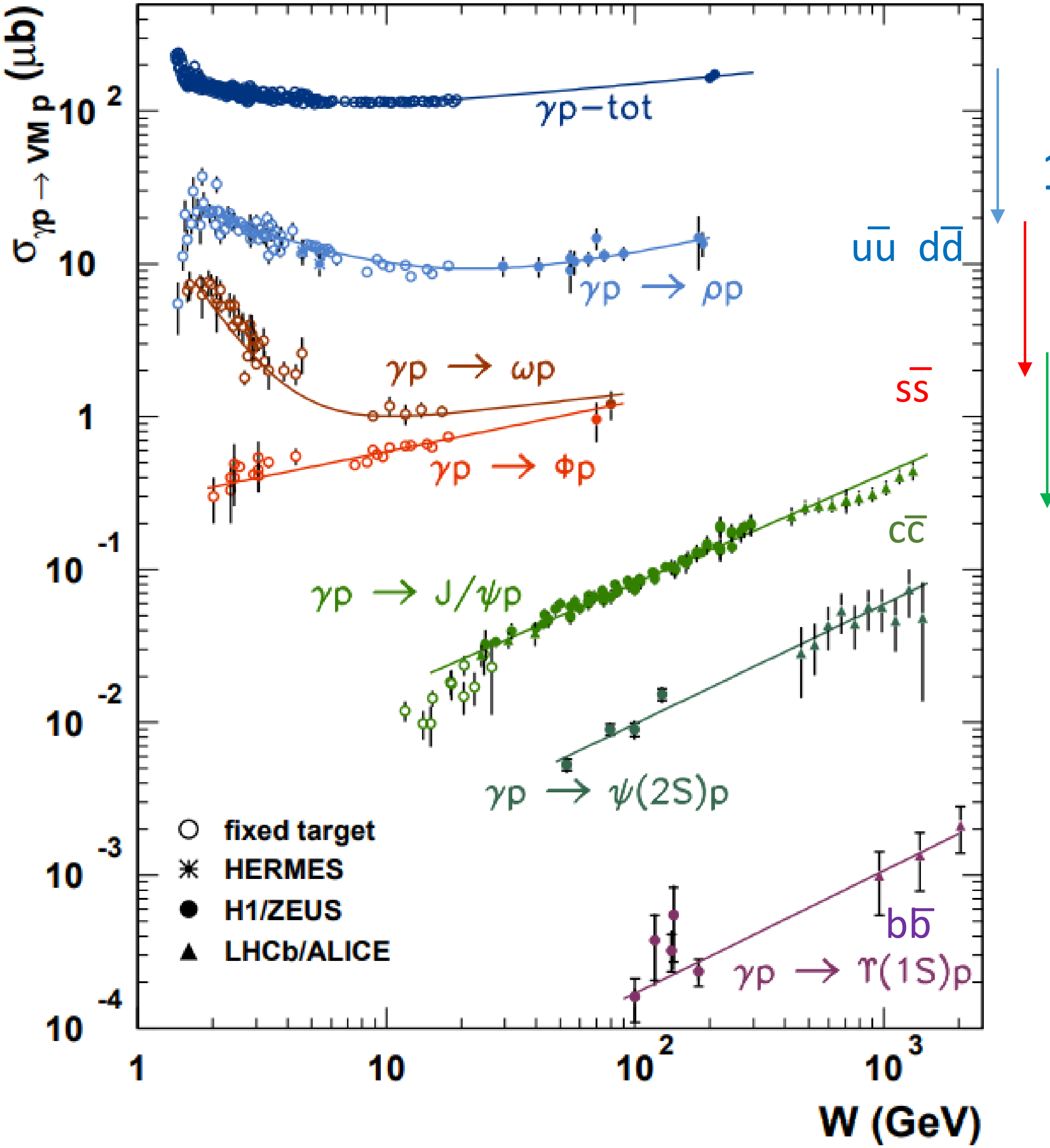

1 order of magnitude

1 extra order of magnitude

1 extra order of magnitude

Still 3 extra orders of magnitude

Exclusive reactions have small cross section

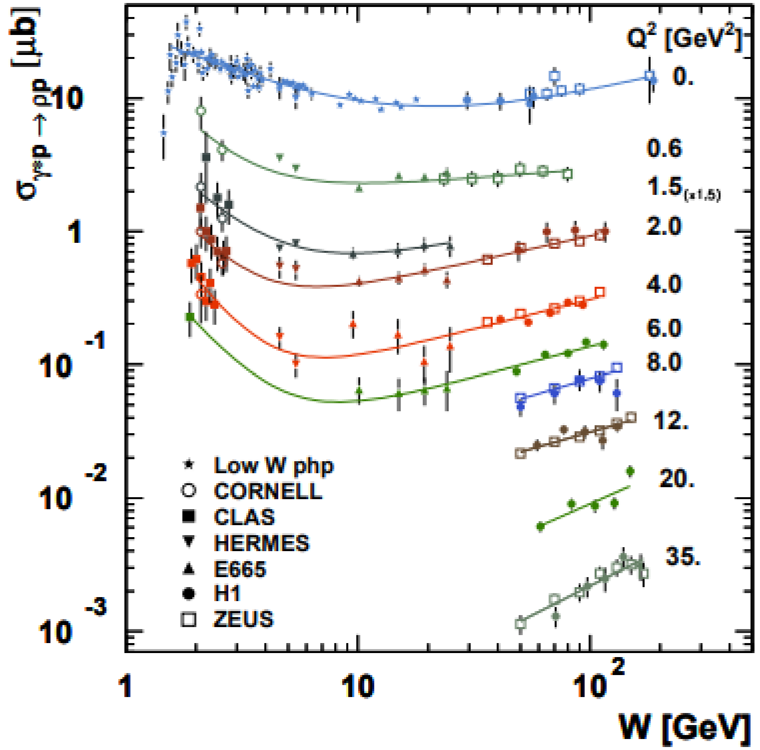

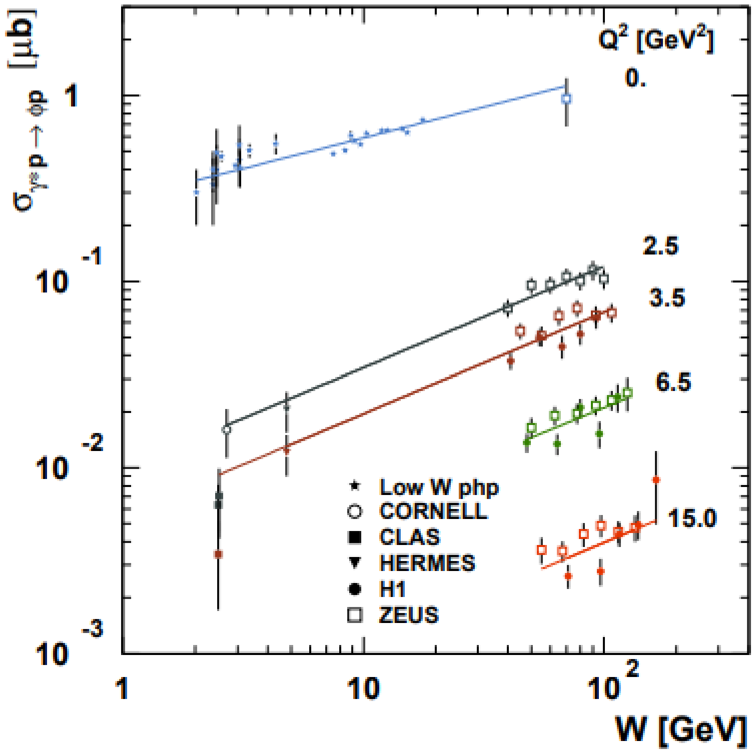

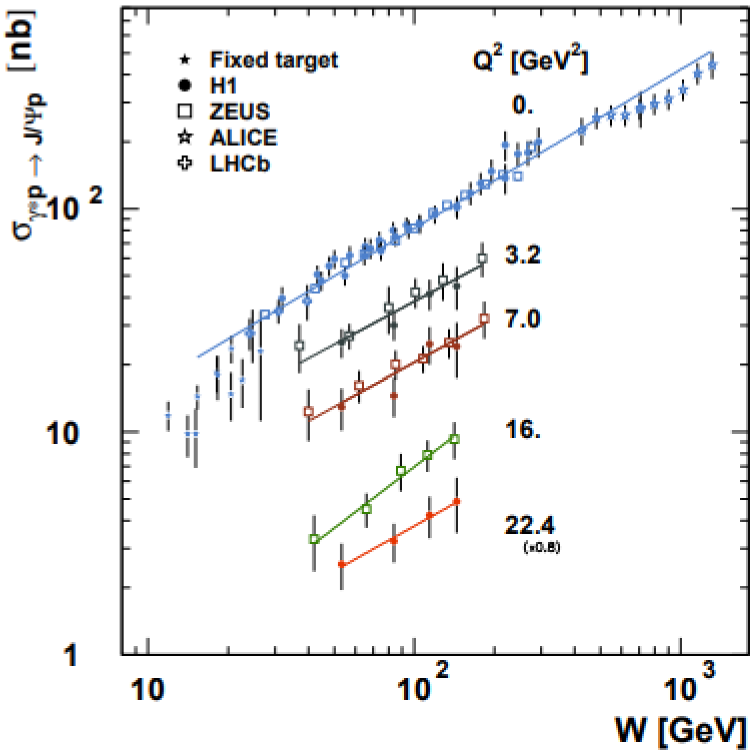

Searching for a needle in a haystack

Selection of the exclusive process among many other competing processes

➔ difficult experiment which need a **very comfortable luminosity**

2 kinds of experimental topology

Fixed target experiment

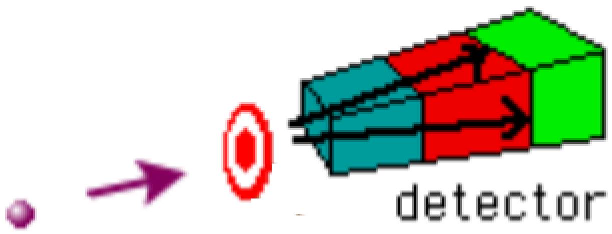

Collider experiment

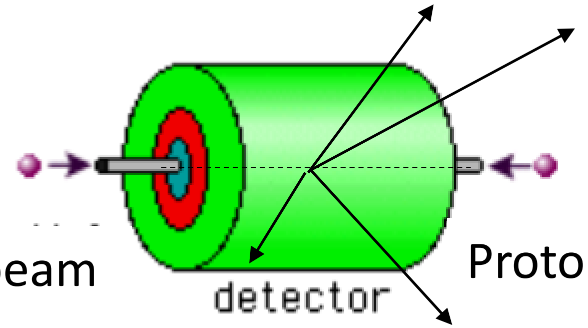

- (Invariant mass)^2 of the lepton-proton system (ℓ-p)

  $s = (k+p)^2 = 2\,k.p$ if $M_\ell << M_p <<$ Energies of the beams

$s = 2\,M_p\,E_\ell$

Ex: COMPASS muon beam E_ℓ =160 GeV $\sqrt{s}$= 17 GeV
Jlab electron beam E_ℓ =12 GeV $\sqrt{s}$= 4.7 GeV

$s = 2\,(E_\ell.E_p - \vec{P}_\ell.\vec{P}_p) = 4\,E_\ell\,E_p$

Ex: EIC electron proton
E_ℓ =18 GeV E_p = 275 GeV $\sqrt{s}$= 140 GeV
E_ℓ = 5 GeV E_p = 100 GeV $\sqrt{s}$= 45 GeV

- Small transfer t

Slow recoiling proton
Difficult to escape the target

Very forward fast proton
Close to the outgoing proton beam

Past and future experiments for DVCS ℓp→ ℓ'p'γ

Fraction of the electron energy carried by the virtual photon

$$y = \frac{p.q}{p.k}$$

$Q^2 \approx s.x_B.y$

$Q^2 \approx 2M_p E_\ell .\ y\ .\ x_B$

or $4\ E_p\ E_\ell .\ y\ .\ x_B$

$0.01 < y < 0.95$

- Small y resolution pb
  $y = \upsilon/E = (E-E')/E$
- Large y radiative corrections

Higher s allows to investigate smaller value of x_B

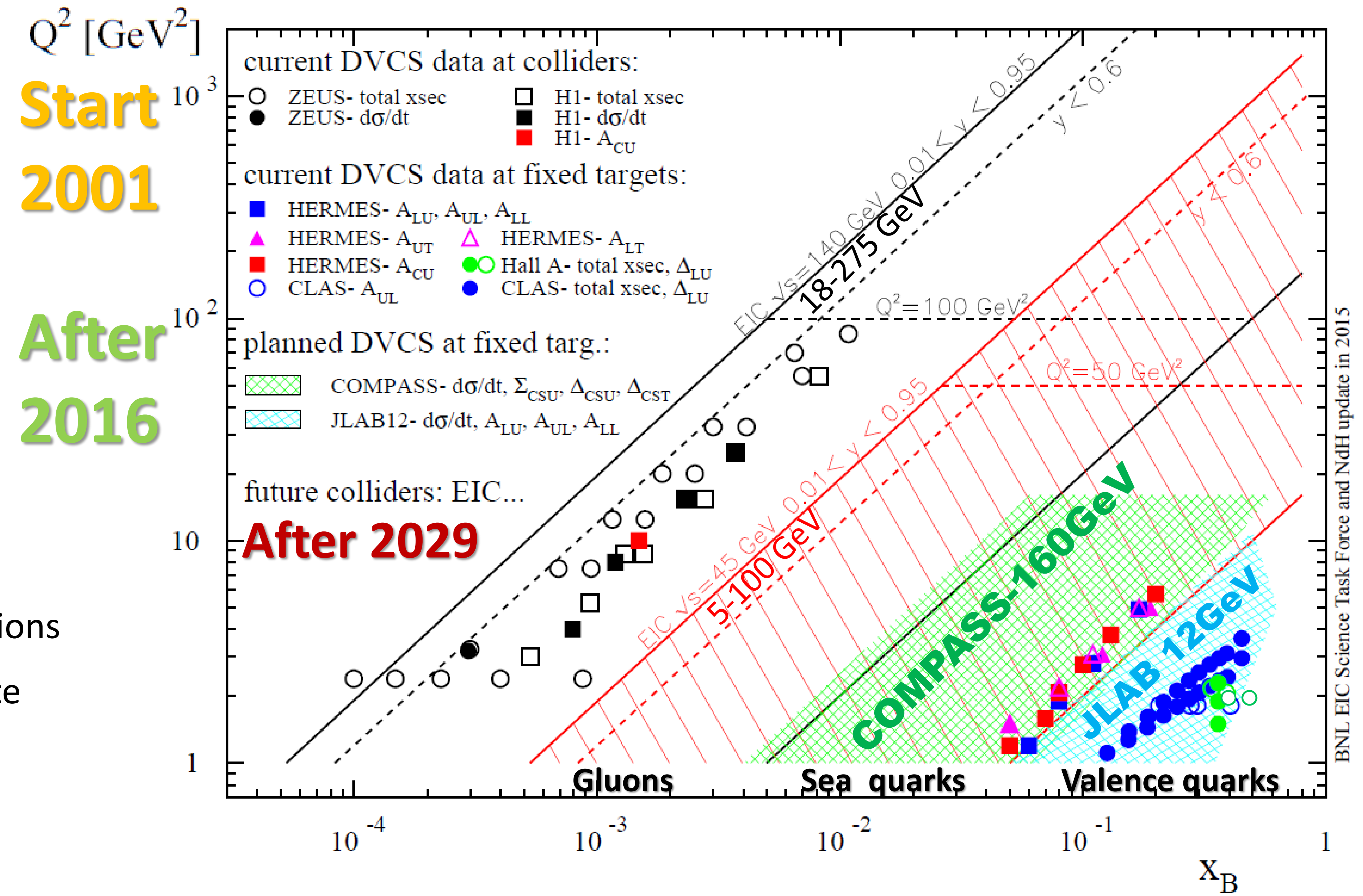

Past & present for exclusive experiments at small t: $\ell p \rightarrow \ell' p' \gamma$ or meson

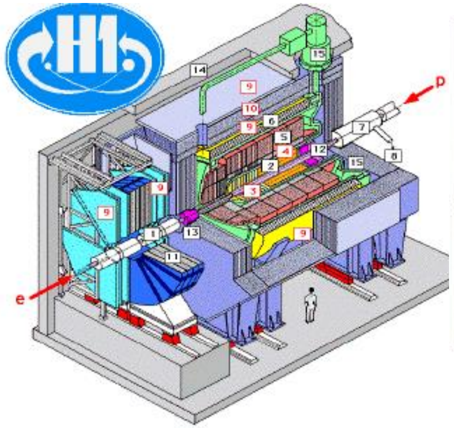

Collider mode e-p: forward fast proton

HERA: **H1** and **ZEUS**
Polarised **27 GeV** e-/e+
Unpolarized **920 GeV** proton
~ *Full event reconstruction (proton in Roman Pots)*

Fixed target mode: slow recoiling proton

HERMES: Polarised **27** GeV e-/e+
Long, Trans polarised p, d gaz target
Missing mass technique
2006-07 with recoil detector

Jlab: Hall A, C, CLAS, CLAS12 High Luminosity Polar. **6** & **12 GeV e-**
Long, (Trans) polarised p, d liquid target
Missing mass technique (A,C) and complete detection (CLAS)

COMPASS @ CERN: Polarised **160 GeV μ+/μ-**
p target, (Trans) polarised target
with recoil detection

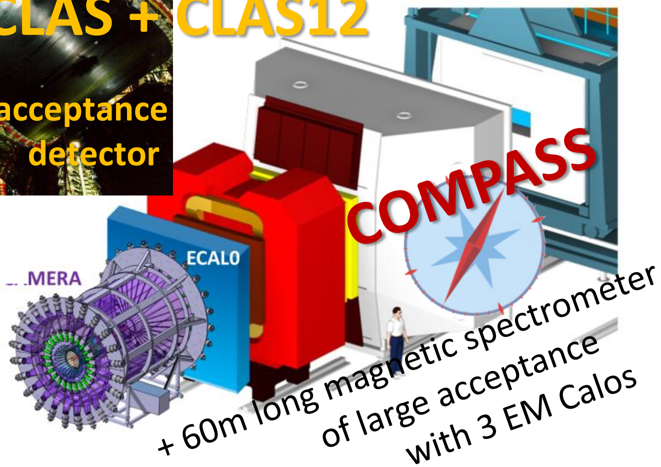

➔ ***Rejection of background: SIDIS, exclusive π^0/DVCS, dissociation of the proton***